Heliyon 8 (2022) e10368

Contents lists available at ScienceDirect

Heliyon

journal homepage: www.cell.com/heliyon

Research article

Envisaging the actual evapotranspiration and elucidating its effects under climate change scenarios on agrarian lands of bilate river basin in Ethiopia

Abera Shigute Nannawo [a,*], Tarun Kumar Lohani [b], Abunu Atlabachew Eshete [a]

[a] Faculty of Water Resources and Irrigation Engineering, Arba Minch Water Technology Institute, Arba Minch University, P.O. Box 21, Arba Minch, Ethiopia
[b] Faculty of Hydraulic and Water Resources Engineering, Arba Minch Water Technology Institute, Arba Minch University, P.O. Box 21, Arba Minch, Ethiopia

ARTICLE INFO

Keywords:
Actual evapotranspiration
Climate change
RCPs
WetSpass-M model
Bilate river bain

ABSTRACT

The earth's natural water and energy systems rely on actual evapotranspiration (AET). Climate change plays a crucial role in affecting the hydrologic processes of Abayya-Chamo lake basin in Ethiopia's Rift Valley, resulting into a distributed actual evapotranspiration (DAET) system. Various studies have already been undertaken on the effects of climate change (CC) on AET but forecasted precipitation and temperature to determine space-time distribution of AET across the basin have not been studied yet. Estimates for precipitation and temperature were acquired from the Coordinated Regional Climate Downscaling Experiment (CORDEX) Africa platform, using RCP4.5 and RCP8.5 scenarios, during 1986–2015, 2041–2070, and 2071–2100 periods. WetSpass-M model was employed to investigate seasonal and annual DAET under varied climate amplitude and distribution. For the baseline period (1986–2015), the maximum annual AET was predicted to be 2815.8 mm/yr. For 2041–2070, and 2071–2100 periods, the estimated maximum annual AET for RCP4.5 scenarios was 3019.2 and 3212.1 mm/yr, respectively, while for RCP8.5 scenarios, it was 3116 and 3352.2 mm/yr, respectively. The baseline annual AET was 516.6 mm/yr, while the mid-term (RCP4.5 and RCP8.5) and long-term (RCP4.5 and RCP8.5) models predicted mean annual AETs of 423.8 and 432 mm/yr and 429.6, and 438.5 mm/yr, respectively. Between 2041 and 2070, the RCP4.5 and RCP8.5 scenarios predicted a 92.8 and 84.6 mm/yr decrease in mean annual AET, respectively. The model predicted a decline in mean annual AET of 87 and 78.2 mm/yr for both scenarios in 2071 and 2100, respectively. With the exception of the basin's maximum AET, the mean annual AET for both RCP4.5 and RCP8.5 emission scenarios may decline during 2041–2070 and 2071–2100. As rainfall declines and temperature rises and the projected AET in the basin gets disrupted in the future decades. This research may add information to the water management and utilization, and a better knowledge of how climate change directly affects AET systems.

1. Introduction

Actual evapotranspiration on natural water and energy systems incurs climate change (CC) affecting the hydrologic processes in the Bilate river basin, resulting in a DAET system. Recurring change in global climatic conditions are expected to have an impact on water systems and other natural biological consequences (Yagbasan, 2016). African ecosystems is affected the most, aggravating the existing water shortage, with long-term consequences expected to be significant and long-lasting not only in the present decade but also the decades to come (Niang et al., 2014; Osima et al., 2018; Nhemachena et al., 2020). The difference in average surface temperature between 2 °C and 1.5 °C global warming levels (GWLs) is greater than 0.5 °C, reaching to 0.8 °C in most of the parts of Sudan and northern Ethiopia (Osima et al., 2018). Under RCP8.5, potential evapotranspiration (PET) in Ethiopia's upper blue Nile basin may increase by 27% by the end of the century, while forecasted water availability in the basin is expected to fall by -1.7 to -6.5% and -10.7 to -22.7%, respectively, due to ongoing climate change (Liersch et al., 2018). For the period 2015 to 2050, the A1B scenario, with a balanced emphasis on all energy sources and the B1 scenario, prioritizes global solutions to economic, social, and environmental sustainability, ultimately led in 13 and 14 % losses in surface runoff, respectively (Gebremeskel and Kebed, 2018). The maximum temperature in Ethiopia's Addis Ababa area would rise to 2.06 °C (CGCM3A2) by 2080, while the minimum temperature would be 1.03 °C (Feyissa, 2018). According to Alehu et al. (2021) the 2020s, 2050s, and 2080s estimates a decrease in rainfall

* Corresponding author.
E-mail address: aberashigute@gmail.com (A.S. Nannawo).

https://doi.org/10.1016/j.heliyon.2022.e10368
Received 22 March 2022; Received in revised form 1 July 2022; Accepted 15 August 2022
2405-8440/© 2022 The Author(s). Published by Elsevier Ltd. This is an open access article under the CC BY-NC-ND license (http://creativecommons.org/licenses/by-nc-nd/4.0/).

amount in all months, particularly in February and May, in the Rift valley's Gidabo catchment, under both RCP's emission scenarios. The continual rise in air temperature compared to the pre-industrial age due to global warming will have an impact on AET (Dimitriadou and Nikolakopoulos, 2021). Average temperature is predicted to rise in various watersheds (Gemitzi et al., 2017; Kahsay et al., 2018; Saatloo et al., 2019; Hughes et al., 2021; Tigabu et al., 2021). AET in the Middle East and North Africa is expected to increase up to 0.3 (~2) mm each year before 2050 (Ajjur and Al-Ghamdi, 2021). DAET assessments for river basins of Bilate river systems have not been undertaken on a regular basis, despite Ethiopia's continually changing climatic conditions. Walraevens et al. (2009) conducted study on a small hill watershed in Ethiopia's northern region. The spatial and temporal variability of AET, as well as its responses to changing climate, were investigated in the Geba and Kliti river systems in Northern Ethiopia (Yenehun et al., 2017), surface and groundwater recharge, including AET, in Ethiopia's Abaya Chamo Basin were modeled (Molla et al., 2019), the implications of CCs on AET and groundwater recharge in the Tekeze basin were assessed (Kahsay et al., 2018), and water budget components within the Bilate river system, including AET have been examined (Nannawo et al., 2021).

Global circulation models (GCMs) and the CORDEX frameworks are the most extensively utilized physically-based tools for constructing diverse climate scenarios (Elshamy et al., 2009). Numerous researchers have improved findings in terms of CC, variability, and its influence on the hydrologic cycle among a number of Ethiopian watersheds using a general circulation model derived from multiple sources (Haile & Tom, 2015; Tekle, 2015; Eromo et al., 2016). GCMs, on the other hand, are unsuitable for local climate impact assessments due to their lack of spatial resolution and inability to capture local effects (Navarro-Racines et al., 2020). As a result, regional climate models (RCMs) have been used to disaggregate global climate model (GCM) data in order to overcome these constraints (Eden et al., 2014). Despite the fact that RCM projections are more precise in terms of geography and time than GCM projections, temperatures and rainfall estimates are still erroneous (Berg et al., 2012).

While climate models can predict future rainfall and temperatures but a significant difference and uncertainty in rainfall forecasts (Kiesel et al., 2019) are the dominating factors. The majority of previous CC studies in the Lake Tana area (Ademe et al., 2020) used single GCMs based on CMIP3 data. The CMIP3 model outputs, on the other hand, have a coarse high spatial resolution that is not at par to the CMIP5 prediction (Taylor et al., 2012). According to CMIP5, climate models may simulate bio-geological systems, aerosols, and carbon cycles, which all contribute to physical climate (Stocker et al., 2013).

AET or the volume of water evaporated and transpired under current climatic circumstances in a specific location, is difficult to quantify (Dimitriadou and Nikolakopoulos, 2021). A WetSpass-M model can be used to calculate AET and variability for different geographical regions throughout the world. The AET in Belgium's Grote Nete Basin was studied using the WetSpass-M physically based and regionally dispersed water budget model (Wang et al., 1996; Batelaan and Smedt, 2001). The methodology is presently being used to calculate AET in some Ethiopian locations (Meresa and Taye, 2019). The findings revealed that having a thorough understanding of a watershed's AET is critical for sustainable water resource management. According to a variety of studies conducted within the Bilate basin by several researchers, CC seems to have the power to alter the frequency and amount of AET through modifying the threats of water scarcity, droughts, and flooding. A few researches on the effects of climate change (CC) on AET have previously been conducted, but projecting precipitation and temperature in order to determine the space-time distribution of AET across the basin have not been investigated yet. As a result, physically based and fully distributed hydrological model WetSpass-M as well as predicted climatic projections was used to solve these problems in the basin. The primary objective of this research is to develop a clear understanding of a basin's AET, which is crucial for long-term water resource management, by estimating the mean seasonal and annual DAET under climate change scenarios.

2. Materials and methods

2.1. Study area descriptions

The Bilate river system drains roughly 5402.8 km^2 in Ethiopia's Central Main Rift between 37^{0}40′ and 38^{0}20′ E longitude (Figure 1), with a semi-arid ecosystem throughout the lower basin and a temperate climate mostly in central, northern, and southwest mountains dominated by agricultural ecosystems, particularly rainfed agriculture with limited irrigation facility (Nannawo et al., 2021). The basin is divided into three geomorphologic zones: rift, escarpment, and highland (Haji et al., 2018). Due to diverse topographical features ranging from 1116 m in the lower reach of the base to 3355 m above mean sea level in the northern Gurage highlands (Figure 1), the mean annual rainfall varies substantially (Ayele et al., 2022; Edamo et al., 2022; Ukumo et al., 2022; Nannawo et al., 2022). The basin is divided into three sub-basins in terms of rainfall distribution, with yearly rainfall of high, moderate and low. Annual rainfall in the high, middle, and lower parts of the river ranges from 1280-1339, 1061–1771, and 769–956 mm, respectively, with an average of 1165 mm for the entire basin (Hussen et al., 2018).

2.2. The WetSpass-M model's input data

The WetSpass-M model requires spatial and temporal data to simulate the magnitude and distribution of AET. The spatial data include the digital elevation model (DEM), slope generated from the DEM, soil texture, and land cover data, while the climatic data (historical and projected precipitation) used in the modeling process were average temperature, wind speed, potential evapotranspiration (PET), static groundwater level and streamflow data from Bilate river. In an ArcGIS environment, all the listed data were produced and provided as inputs to the WetSpass-M model (Kahsay et al., 2018). The basin's highest point was 3355 m above mean sea level (a.m.s.l.) in the northern Gurage Mountains, while its lowest point was 1116 m at the basin's outlet. Using ArcGIS′ slope analysis tool, the terrain map is generated from the DEM. The slope ranges between 0% and 216.8%. The basin has been experienced a bi-modal rainfall distribution patterns of climatic zone (McSweeney et al., 2010) comprising of winter, summer and spring. The WetSpass-M model is used to simulate the hydrological processes within a climate-changed basin, and it shows a significant effect of CC on DAET in this basin from a multi-method perspective (Woldeamlak et al., 2007; Nyenje and Batelaan, 2009; Haile & Kassa, 2015; Yenehun et al., 2017) (Figure 2).

2.2.1. Land use

Land-use statistics for 2020 were compiled using Landsat 8 data (Path 168, 169 and Row 054, 055, and 056). From the ASTER elevation archives, the Ethiopian Geological Mapping Agency provided a DEM with a resolution of 30 m and an elevation grid map with a resolution of 30 m. Landsat data was obtained in January to help alleviate the cloud situation. Once the data were available, ENVI 5.3 software was used to process and categorize it via the maximum likelihood (ML) pixel-based trained classification technique. The producer's accuracy, which seems to be a measure of how accurately actual land classes can indeed be classified, is used to calculate omission errors. The statistics for open-water, settlement, agricultural-land, forest-area, shrub-land, grassland, and barren-land are 115, 450, 3286, 490, 345.4, 377, and 337 (km2), respectively. According to the report, agricultural regions dominate land usage in the Bilate river basin (Figure 2a).

2.2.2. Soil types

A soil texture map of the Bilate basin was produced using the FAO's harmonized information from 1998 (Figure 2b). Using the hydraulic characteristics, conversion of the soil moisture aspects tool, soil groups were transformed to USGS texture classes assuming topsoil percentages of grain sizes fractions to conform the model parameters. 2337 km^2 of the basin is covered by loam, sandy loam 2246 km^2, clayey sand 816 km^2, and loamy sand 2 km^2 which are depicted on the modified textural map.

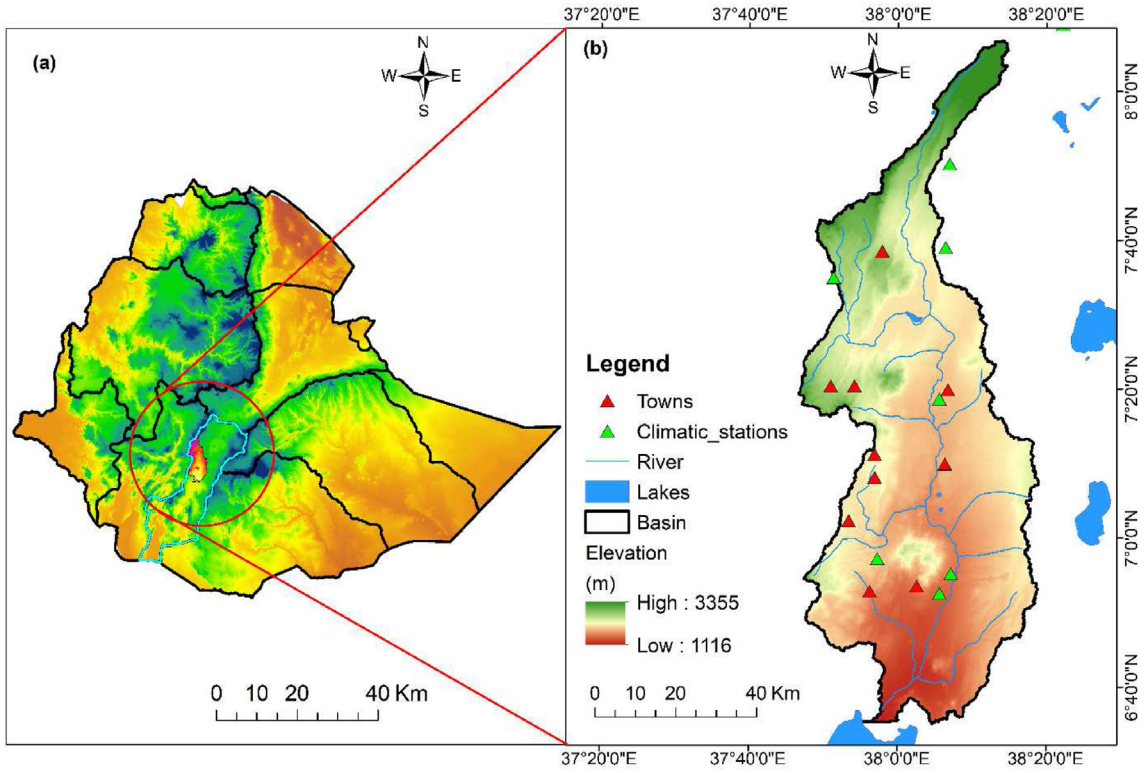

Figure 1. The study area: a) river basins of Ethiopia, b) Bilate river basin.

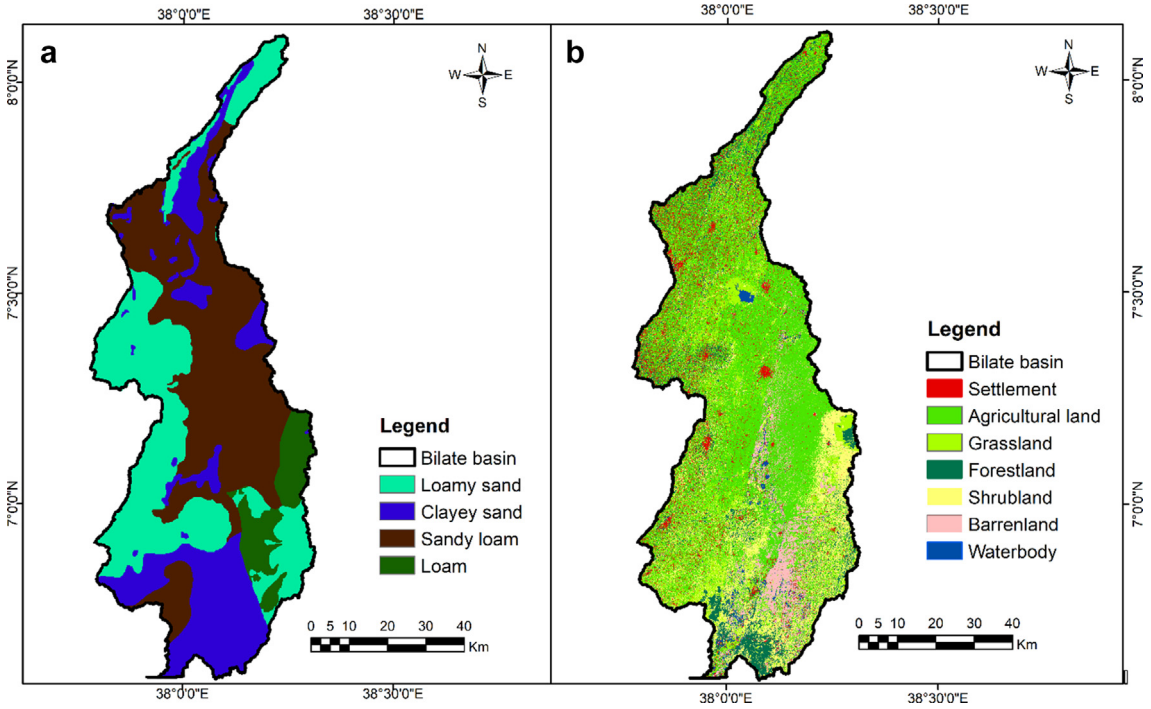

Figure 2. Soil and Land use map of Bilate river basin. Note: a) = soil textural, b) = land use map.

2.2.3. *Potential evapotranspiration (PET)*

PET is one of the important inputs for WetSpass-M model (Woldeamlak et al., 2007; Jarosław and Batelaan, 2011; Yenehun et al., 2017). Enough climatic data, such as mean air temperature, maximum and minimum air temperature, relative humidity, downward long-wave and short-wave radiation flux, upward long-wave and shortwave radiation flux, wind, sunshine hour, and altitude (elevation) are required to estimate potential evapotranspiration using Penman-Monteith methods (FAO, 2007). The majority of meteorological stations, with the exception of Hosanna and Alaba-kulito, give insufficient data, such as relative humidity, wind speed, and sun radiation. As a result, for stations with complete data, evapotranspiration was calculated using Penman-Monteith methods and Hargreaves equations (**Eq.** 1) for the mean daily minimum and maximum temperature and extraterrestrial

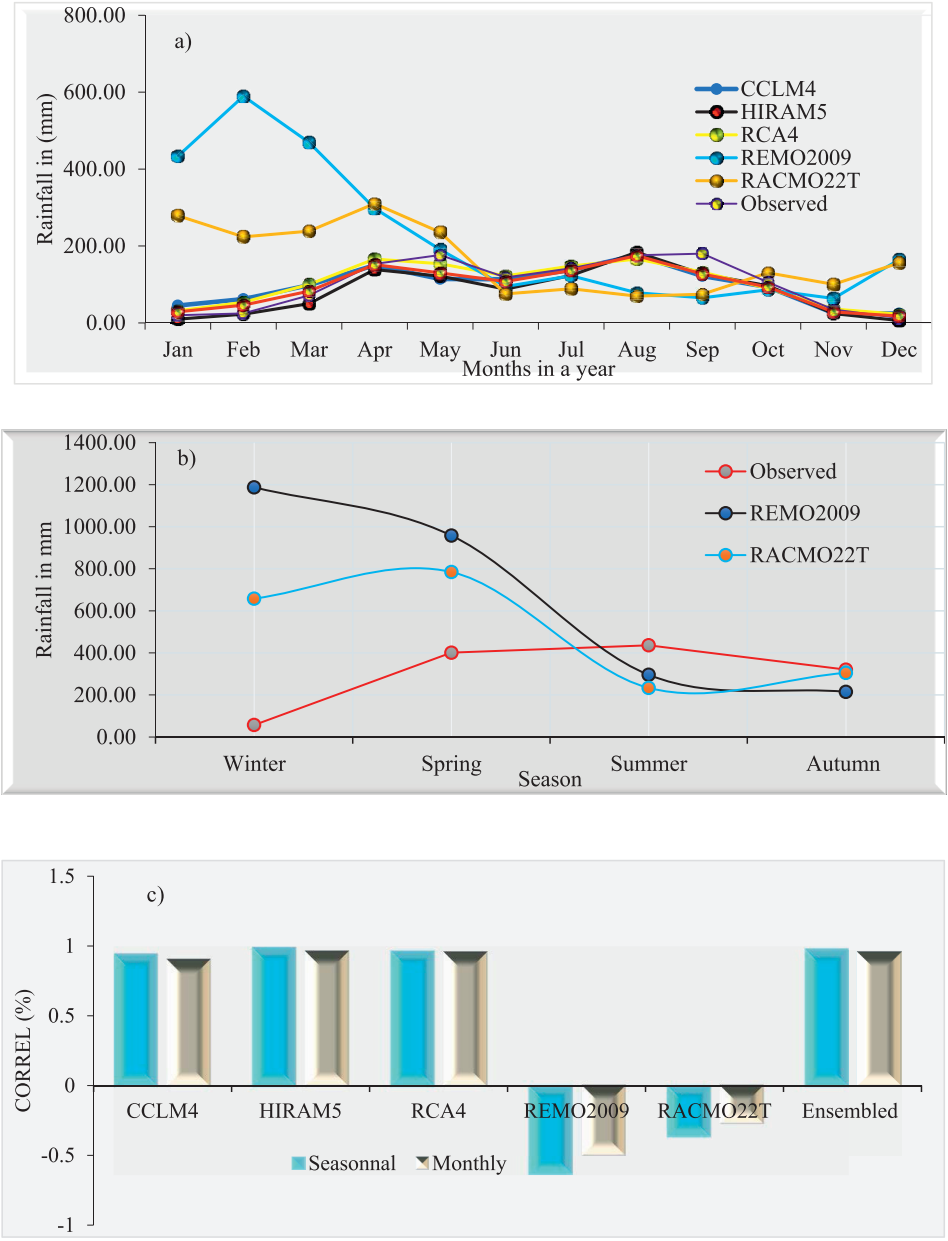

Figure 3. Rainfall distribution for all observed and downloaded climatic data and correlation coefficient. Note: a) Mean monthly projected and observed rainfall data, b) Mean seasonal projected and observed rainfall data, c) correlations between projected and observed mean monthly and seasonal rainfall.

radiation, and the estimated evapotranspiration was used as an input to the WetSpass-M model (Allen et al., 1998).

$$PET = 0.0023\ (T_{mean} + 17.8)\ (T_{max} - T_{min})^{0.5}.R_{a,} \quad (1)$$

PET = the potential evapotranspiration (mm/day), Tmax, Tmin and Tmean are projected maximum, minimum and average temperature (0C) for RCP scenarios, respectively.

R_a is extraterrestrial radiation (mm/day), The corrected average daily PET, precipitation and observed stream discharge was provided as an input for the WetSpass-M model to simulate the water balance processes and evaluate the magnitude and distributed groundwater recharge value under land use and land cover (LULC) and changes in climate in the Bilate sub-basin.

2.3. Projected rainfall and temperature

Projected climatic data (precipitation and temperature) were obtained in NetCDF format from the Coordinated Regional Climate Downscaling Experiment (CORDEX) Africa platform for the periods 1986–2015, 2041–2070, and 2071–2100 using RCP4.5 and RCP8.5 scenarios. As a result, the RCP Scenarios included in this study have been classed as RCP4.5, with RCP8.5 expected after 2100 (Worku et al., 2020; Rahimpour et al., 2021). MPI-CCLM4, ICHECHIRAM5, ICHEC-RACMO22T, CNRMRCA4, and MPI-REMO2009 outputs were also used. Downscaled values cannot generally be used for effect evaluation since the projected elements may differ significantly from the recorded data (Mutayoba and Kashaigili, 2017). The most popular techniques for predicting the consequences of global warming are general circulation models (GCMs), although their level of errors and uncertainty makes it difficult to simulate real climatic occurrences (Green et al., 2011; Cannon et al., 2015; Bekel et al., 2021; Kumar et al., 2021; Mengistu et al., 2021; Ukumo et al., 2022). GCM simulations have enormous errors when compared to historical data. The bias reduction was used for the possibility that downscaled parameters might exaggerate or underestimate the actual mean, and the basic climate model outputs were modified through

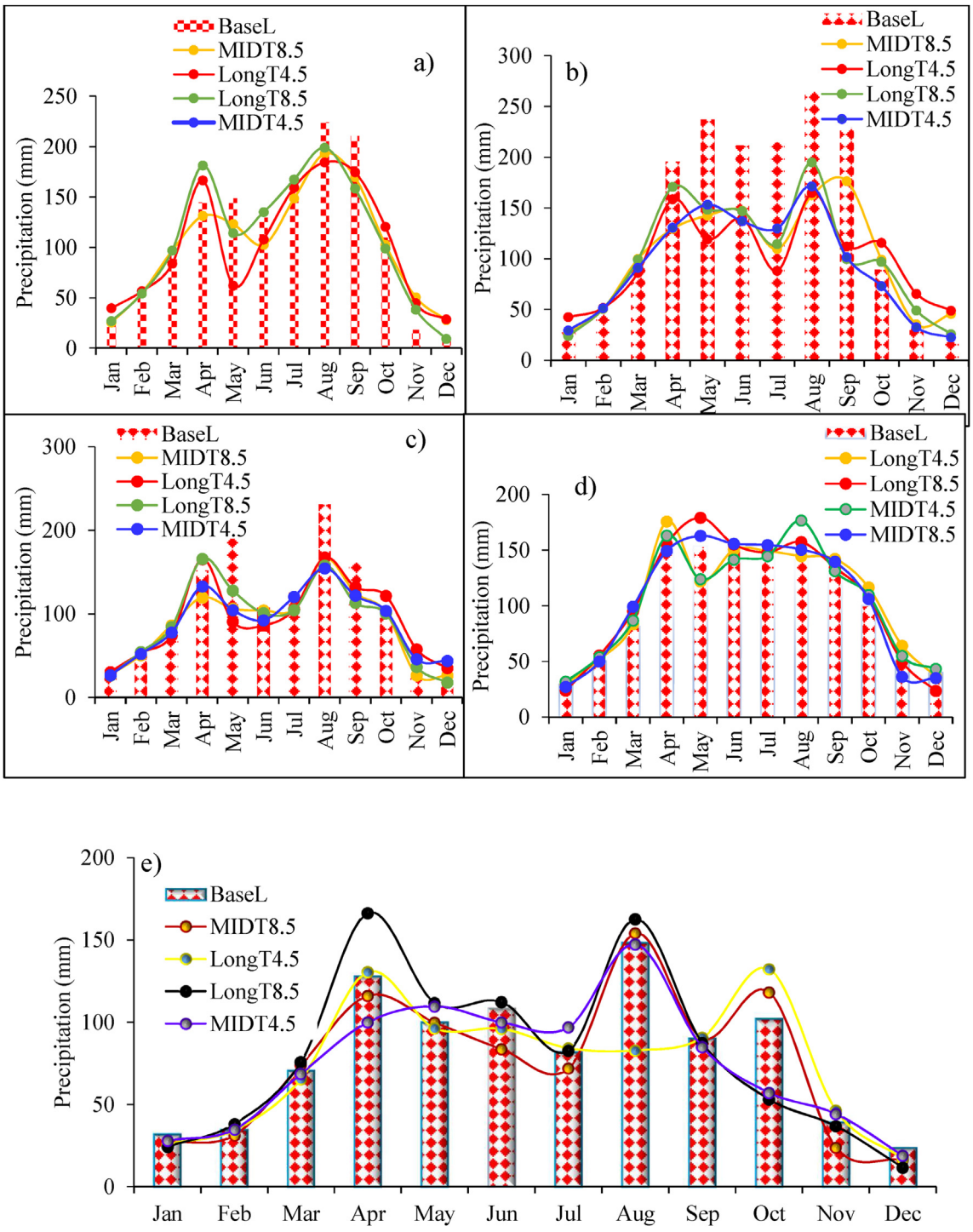

Figure 4. The mean monthly ensemble mean of predicted rainfall. Note: a) = Hulbarag, b) = Hossana, c) = Alaba-Kulito, d) = Boditi, and e) = Bilate-Tena weather stations, BaseL. = Base Line periods, MIDT4.5 = Mid-Term RCP4.5 (2041–2070), MIDT8.5 = Mid-Term RCP8.5 (2071–2100).

bias corrections to provide a more accurate climatic projection that closely reflects the future impact of climate change.

2.4. Bias corrections

Climate model data can differ greatly from actual data or data acquired from gauging stations. This errors are corrected before using CC scenario data throughout hydrological effect evaluations (Berg et al., 2012). Temperature linear scaling (pLS), rainfall linear scaling (pLS), and rainfall power transformation are examples of biased efficacy controls that used in this study (**Eq.** 2). Figure 4 shows the use of climate scenario data to compare observed data to monthly average rainfall (1986–2015). The monthly ensemble means of predicted rainfall at the climatological stations at Hulbarag, Hossana, Alaba-Kulito, Boditi, and Bilate-Tena were computed using RCP4.5 and RCP8.5 greenhouse gas emission scenarios (Figure 4a–e) (Hughes et al., 2021; Tigabu et al., 2021; Edamo et al., 2022; Ukumo et al., 2022). The observed data from the same was compared to the historic model data from 1986 to 2015. Statistical metrics such as percentage relative bias (PBIAS) (**Eq.** 3), mean absolute error (MAE) (Eq. 8), Pearson correlation coefficient (r) (Eq. 4), and root

mean square error (RMSE) (Eq. 9) are used to evaluate performance of the model. Pearson correlation coefficient is used to evaluate the linear relationship between the observed and modeled rainfall amounts. The value of 1.0 suggests perfect linear relationship between the model output and observed data (Edamo et al., 2022; Ukumo et al., 2022)

$$P_{bc} = aP_{ob}^{b} \quad (2)$$

The percentage of bias, or PBIAS, is denoted as

$$PBIAS = \frac{\sum_{i=1}^{n}(P_{ob-P_{RCM}})}{\sum_{i=1}^{n}P_{ob}} \times 100\% \quad (3)$$

$$\text{Correlation coefficient, } r = \frac{\sum_{i=1}^{n}(P_{RCM} - P_{RCMavg})(P_{ob} - P_{avg})}{\sqrt{\sum_{i=1}^{n}\left((P_{RCM} - RCM_{avg})^{2}(P_{ob} - P_{avg})^{2}\right.}} \quad (4)$$

R_{RCM} and Pob term represent rainfall amount over the basin from RCM projections or observed data sources from the stations in the basin, respectively; P_{RCMavg} and $P_{obavg\ average}$ projected and observed rainfall respectively in the basin; n, number of samples of rainfall data parameter time series; P_{bc} = bias-corrected projected rainfall, a = transformation coefficient, and b = a scaling exponent.

Due to an unsuccessful fit of bimodal rainfall distribution for all observed climatic stations, ICHEC-RACMO22T and MPI-REMO2009 were removed from the five climate models for the current investigation (Figure 3a). Figure 3a indicates that the RACMO22T model predicted 155.59, 278.82, and 223.66 mm of historical mean monthly rainfall in the basin's dry months from December, January, and February, respectively, whereas the RECMO2009 model predicted 164.26, 433.48, and 589.7 mm. The basin's climatic stations recorded 12.01, 19.79, and 24.59 mm of average rainfall in December, January, and February, respectively (Figure 3a). When comparing the projected monthly rainfall to the observed rainfall from the basin's climatic stations in these months, the projected monthly rainfall was ambiguously high and failed to fit a bimodal rainfall distribution.

During the dry (winter) season, the mean seasonal rainfall for the RACMO22T and RECMO2009 models was 659.07 mm and 1187.43 mm, respectively. On the other hand, the observed average seasonal rainfall for this season was 57.31 mm (Figure 3b) which is very low as compared to the projected values. The distribution patterns of the projected and observed mean seasonal rainfall patterns are notably different. In the summer, the output of the forecasted rainfall from the RACMO22T and RECMO2009 models is comparatively low, whereas the autumn and winter seasons indicate confusingly high in rainfall amounts compared to the observed mean seasonal rainfall. With the exception of RACMO22T and RECMO2009 models' mean monthly and seasonal rainfall, all projected mean monthly and seasonal rainfall shows positive correlations with observed rainfall (Figure 3c). The RACMO22T and RECMO2009 models' projected mean monthly and seasonal rainfall showed negative relationships with observed rainfall in the basin. The monthly correlation coefficient (r) of the RACMO22T and RECMO2009 models to observed historical periods is -0.26 and -0.49, respectively, whereas the seasonal correlation value is -0.36 and -0.63 (Figure 3c). These results imply that the link between observed and model output is weak. On the contrary, the correlation coefficient of other models' outputs, including ensemble mean, with the observed rainfall value ranges between 0.90-0.95 for monthly and 0.94–0.98 for seasonal. These results imply that the link between observed and model output is cohesive. The magnitude and distribution of the AET were determined using MPI-CCLM4, ICHECHIRAM, and CNRMRCA4 outputs. The RECMO2009 model's output specifically does not fit the Gilgel Gibe district's bimodal rainfall distribution pattern (Demissie and Sime, 2021).

2.5. Model evaluation

Statistical measures are employed to determine how well the WetSpass-M model reproduces an observed hydrograph. A good match in the graphs must show that the data and the model for the research region are appropriate. The mean squared error (MSE) (Eq. 5), Coefficient of variation (CV) (Eq. 10), mean absolute error (MAE) (Eq. 8), coefficient of determination, and root mean squared error (RMSE) are all considered in this study. These statistics represent quantitative estimates of the goodness of fit between observed and simulated values, and are used as indicators depicting the model predictions to match the observed. Model prediction capabilities are evaluated based on the results of these tests. The relative and absolute errors in the observed and simulated discharges can be used to assess the goodness of fit: The evaluation criteria employed in this study are as follows:

$$MSE = \frac{\sum_{i=1}^{n}(R_i)^2}{n} \quad (5)$$

$$R_i = S_i - P_{ob} \quad (6)$$

$$R^2 = \frac{RSS}{SST} = -\frac{ESS}{TSS} \quad (7)$$

$$MAE: = \frac{1}{n}\sum_{i=1}^{n}\left|(P_i - O_i)\right| \quad (8)$$

$$RMSE: = \sqrt{MSE} \quad (9)$$

$$CV = \frac{\delta}{\mu} \quad (10)$$

Where; R_i is the residuals (Eq. 6), or estimated errors differences between the observed and simulated data, P_{ob} is observed value and S_i is the simulated value, R^2 is coefficient of determination (Eq. 7), TSS is total sum of the squares, RSS is sum of square of residual, ESS as sum Error of squares. The mean absolute error RMSE is a means of determining how accurate forecasts or predictions are in terms of actual outcomes. The equation $RMSE = \sqrt{MSE}$ is used to calculate the root mean squared error (RMSE) (Eq. 9). MSE stands for mean squared error. For a perfect fit, RMSE = 0 so, the RMSE index ranges from 0 to infinity, with 0 representing the ideal (Mengistu et al., 2021).

3. Results

3.1. GCM-RCM model performance evaluation

The accuracy of the models in generating the observed amount of rainfall in the research domain varied in the current investigation. CNRM-RCA4 has the lowest Bias of -5.7% and the highest CV of 11.6%, indicating the best performance, while MPI-CCLM4 has the highest Bias (−13 percent). In terms of R, the ICHEC-HIRAM5 model was the most successful (0.87). The CNRM-RCA4 CV value (11.6%) is close to the observed value (11.3%), showing that the observed and simulated rainfall had less volatility. With a value of 17.7, the CNRM-RCA4 model is estimated to perform the best in terms of RMSE, while the ICHEC-HIRAM5 model performs the worst (Table 1).

Table 1. Observed vs. RCPs (4.5 and 8.5) dataset performance evaluation.

	Bias (%)	CV (%)	RMSE (mm/year)	r (-)
Gauged	-	11.3	-	-
MPI-CCLM4	-13.0	11.9	20.1	-0.1
ICHEC-HIRAM5	-8.5	19.8	17.0	0.87
CNRM-RCA4	-5.7	11.6	17.7	0.73

3.2. Analysis of projected rainfall

Between 2041 and 2070, the ensemble means rainfall variations across mid-term RCP 4.5 and RCP8.5 scenarios show significant heterogeneity. Rainfall is anticipated to reduce by 3.6%, 9.4%, 0.6%, and 1.51% at Hulbarag, Hossana, Alaba-Kulito, and Boditi stations, respectively, under the RCP4.5 scenario. The predicted total mean ensembled rainfall has decreased in all stations throughout the basin over the long-term RCP8.5 scenario for the twenty-first century 2071–2100 (Figure 5a-e). The highest in annual rainfall recoded decrease (599.98 mm, or 30.5%) is seen at the Hossana station (Figure 5b), while the smallest (3.09 mm) is shown at the Boditi station (Figure 5d). The highest average means ensembled rainfall was at Boditi station, with an estimated value of 18.33 mm over the long-term for RCP4.5 scenarios, and the lowest mean ensembled rainfall was at Bilate-Tena station, with an estimated value of 0.82mm over the mid-term for RCP4.5 scenarios.

Rainfall projections for two time periods of 2041–2070 and 2071–2100 were considered. Seasonal rainfall was predicted to increase in winter seasons across all RCP scenarios during mid-term and long-term periods, with the exception of the RCP8.5 scenario, which was expected to decrease. When using RCP8.5, Hossana station's calculated value of

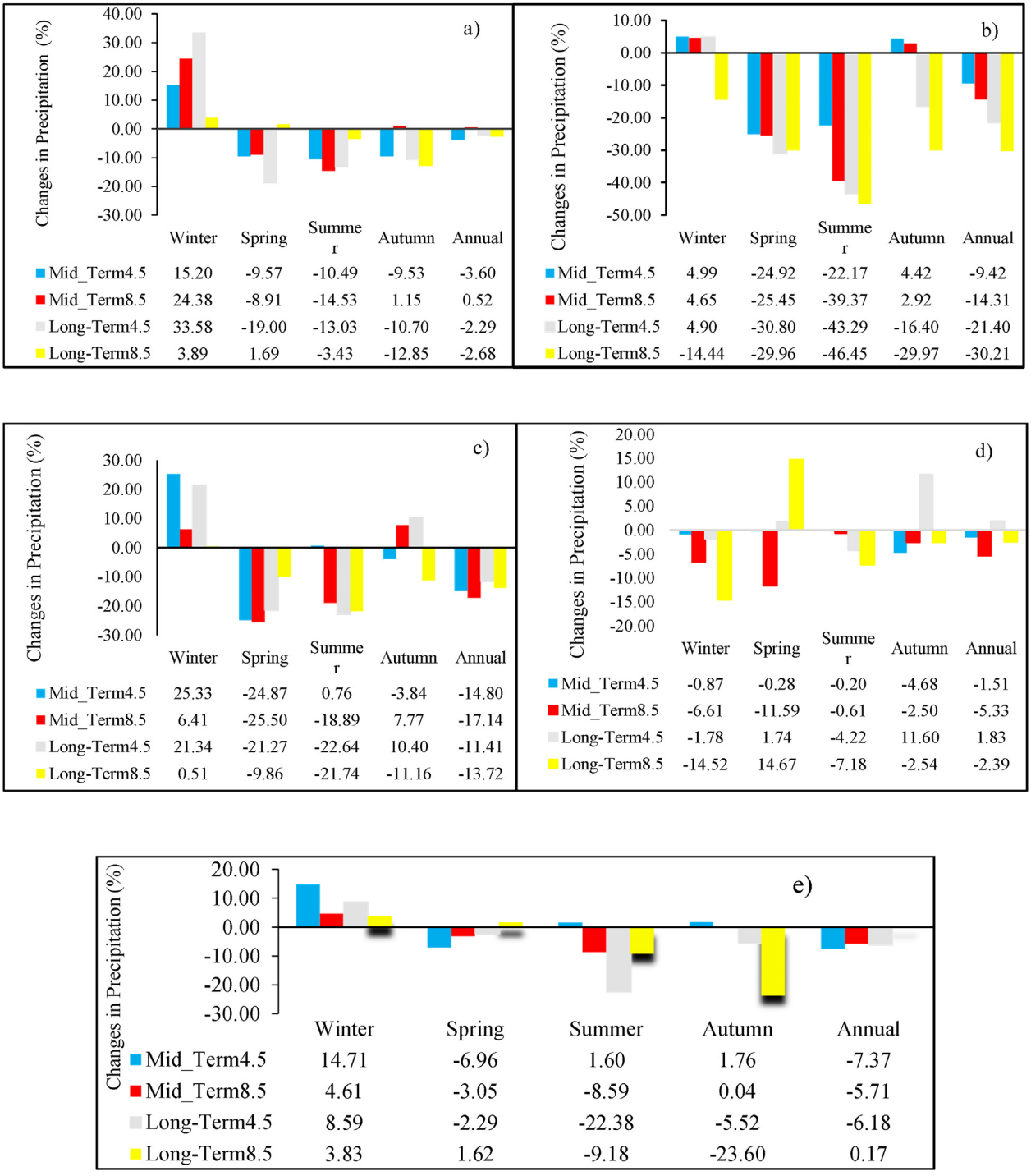

Figure 5. Amount of mean seasonal precipitation variation (mm) for RCP (4.5 and 8.5) scenarios of ensembled mean of CCLM4, HIRAM5, and RCA4 models relative to base period. Note: a) Hulbarag, b) Hossana, c) Alaba-Kulito, d) Boditi, and e) Bilate-Tena weather stations.

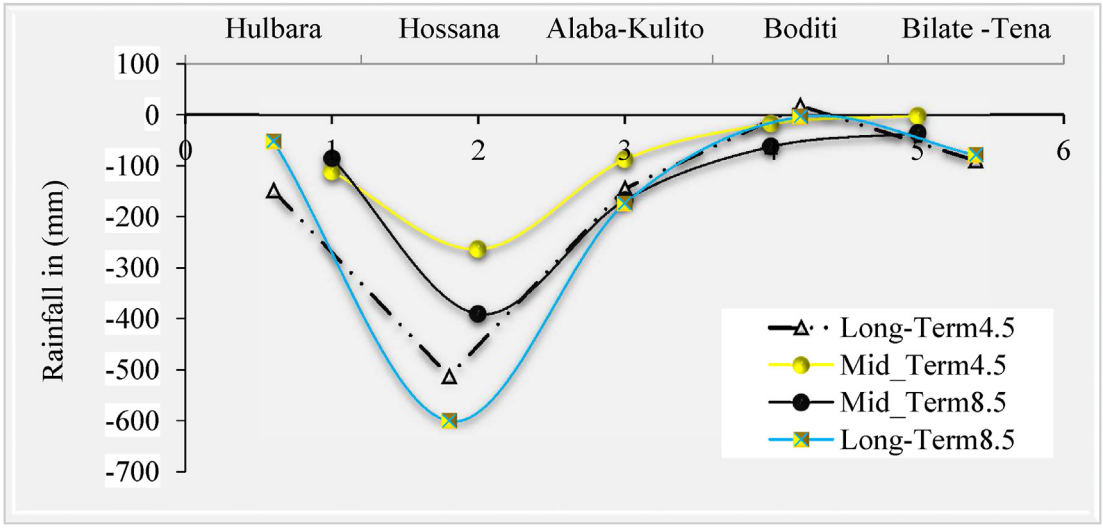

Figure 6. Amount of mean annual precipitation variation (mm).

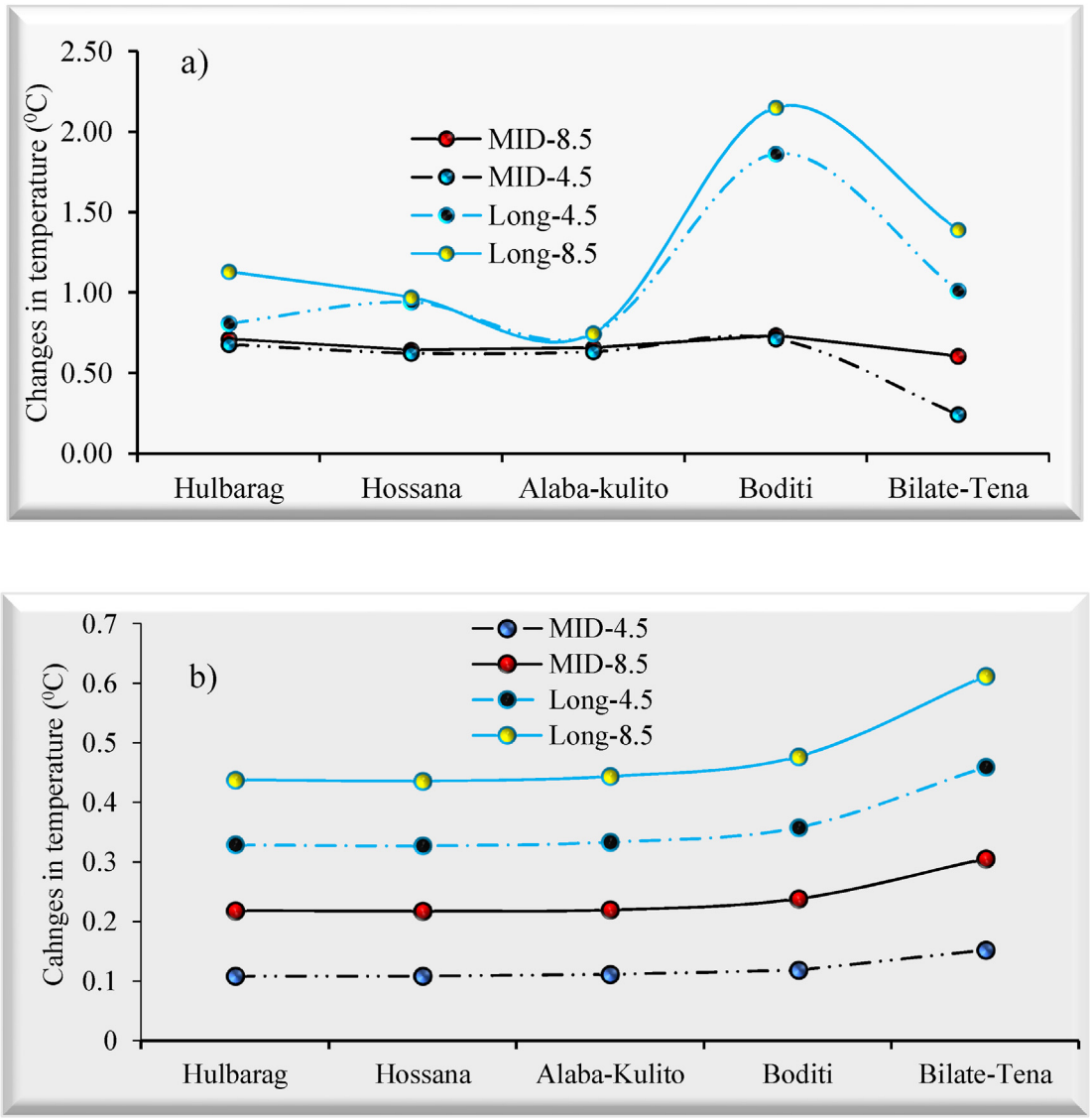

Figure 7. The mean annual temperature changes of at each station of the basin. Note: a) mean minimum temperature b) mean maximum temperature.

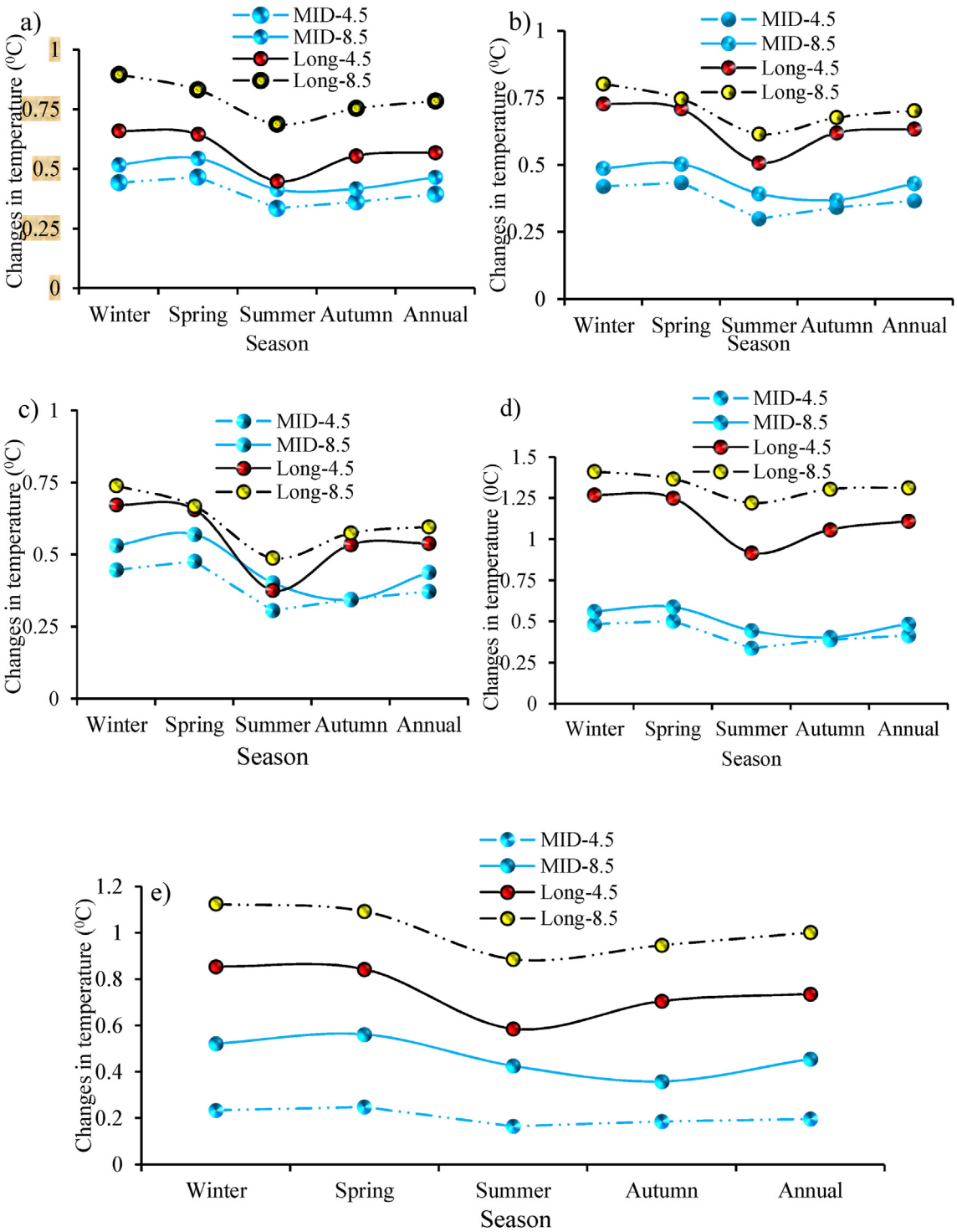

Figure 8. Average (minimum and minimum) seasonal and annual temperature at each station of the basin. Note: a) Hulbarag, b) Hossana, c) Alaba-Kulito, d) Boditi, and e) Bilate-Tena stations.

599.98 mm (30.21%) over the period of 2071–2100 was the highest, and Boditi station's was the lowest (3.09 mm) (Figure 6).

3.3. Projected mean seasonal and annual minimum temperature

In comparison to the base period (1986–2015), the value of average seasonal and yearly minimum temperatures has increased for all stations and all analyzed periods for the assessment periods 2041–2070 and 2071–2100 (Figure 7a-b). In long-term (RCP8.5) scenarios, the biggest percentage rise variation value was 0.61 °C at Bilate-Tena station, whereas the smallest percentage increase in medium-term (RCP8.5) scenarios was 0.11 °C for both stations (RCP4.5). For almost all seasons, the computed seasonal and yearly averaged maximum temperature across all stations shows a consistent rising pattern (Figure 7b). Over the same RCP8.5 scenario, the biggest change in the seasonal maximum temperature of the middle and late periods may continue to rise throughout the winter season. During 2041 and 2070, the mean maximum temperature climbed by 2.15 °C at Bilate-Tena station in Belg

(spring season), but the least rise was 0.75 °C at almost the same place between 2071-2100 RCP8.5 (Figure 7b).

3.4. Mean seasonal maximum and minimum temperature

The average temperature in all the sites will rise regardless of rainfall patterns, as shown in the graph (Figure 8a-e). In RCP4.5 emission scenario, the temperature rises from 0.23 °C in 2041–2070 to 1.27 °C in 2071–2100 during the Belg season. During the long-term RCP scenario, the maximum mean temperature was measured at Boditi station, with a forecasted value of 1.41 °C. In the 2050s and 2080s, the average annual temperature is expected to rise in all seasons in all RCP scenarios. Demissie & Sime (2021) had undertaken the research in the rainfall and temperature simulation capabilities of CORDEX regional climate models like ICHEC-HIRAM5, MPI-CCLM4, and CNRM-RCA4.

3.5. Potential impacts of climate changes on annual AET

3.5.1. Performance of WetSpass-M model

In the WetSpass-M model, calibration is carried out using trial simulation. The model's output is compared with the observed surface-runoff and filtered base flow. Based on the comparisons and evaluations, parameter adjustments are made to improve the model's performance. Figure 9 a and b depicts a comparison of the measured and simulated runoff and base flow from separated discharge using BFI+3 hydro Office tools for the basin. The alpha coefficient, "a" interception, Lp coefficient, average rainfall intensity (I), and runoff delay factor "x" are among the parameters that have been changed in the basin. The surface-runoff and base flow derived by separating the observed river discharge using base flow separator were kept in reserve and optimized until a final agreement was obtained. The model was calibrated using the simulated data from the WetSpass-M model with base flow and surface-runoff. The simulation analysis was acceptable, with correlation coefficients (R^2) of 0.82 and 0.84, and standard errors of 0.32 and 0.42. The parameters were adjusted to the following for goodness-of-fit: average rainfall intensity (I) = 5.8 mm/h (LP) = 1, (a) = 6.4 mm/day, and (x) = 0.37. The WetSpass-M model can predict acceptable total surface runoff and base flow results after calibration.

3.5.2. Changes seasonal AET

The mean seasonal AET across the RCP (4.5 and 8.5) emission scenarios may increase throughout the winter season. The RCP4.5 scenario

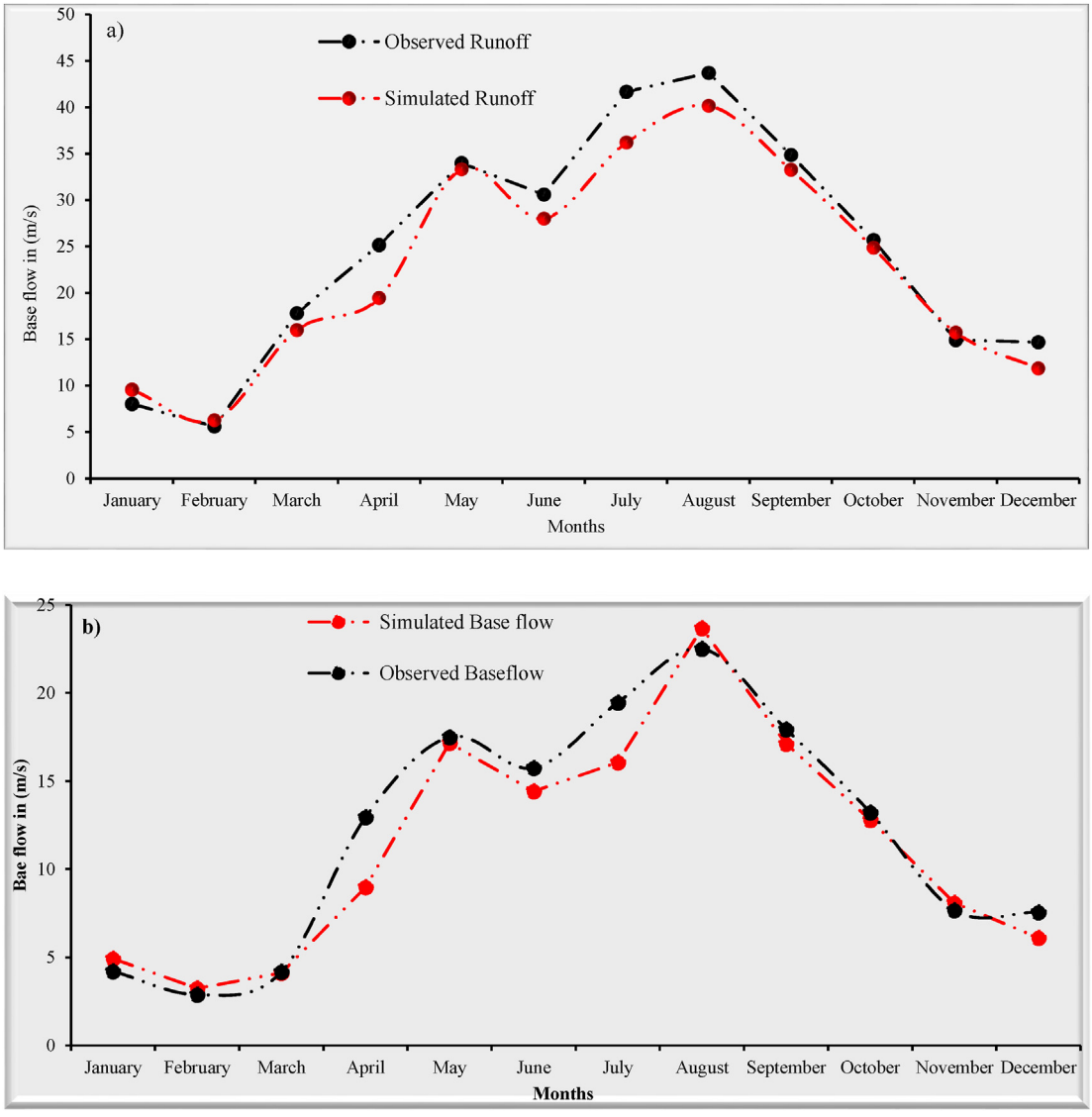

Figure 9. Performance of WetSpass-M model. Note: a) comparison of the direct runoff and simulated runoff, b) comparison of the filtered base flow and simulate base flow.

has the greatest decrease in mean seasonal AET during the periods 2071–2100, with predicted values of 44. mm and 57 mm in the spring and summer seasons, respectively, as seen in the graph (Figure 10c). Future mean seasonal AET might be reduced under the RCP8.5 scenario, with mid-term values of 40.8, 36.4, and 16.6 mm in spring, summer, and autumn seasons, respectively, and long-term values of 15, 16.4, and 27.3 mm in mentioned season respectively. The maximum increase in AET was observed in the spring season with a magnitude of 160.8 mm between 2071-2100, while the maximum decrease in AET was unlikely to be recorded in the same season with a magnitude of 74.4 mm during 2040–2071 as depicted in the RCP8.5 scenario's entire computation period (Figure 10b). Unlike mean and maximum AET, minimum AET increased and decreased the most during the autumn season, with anticipated values of 25.9 and 23.3 mm for RCP (4.5 and 8.5) scenarios throughout the end of 21 century, respectively (Figure 10a). The minimum AET for RCP8.5 emission scenarios declines in all seasons over the mid-term timeframe, with projected values of 7.2, 5.3, 12.5, 4mm in winter, spring, summer, and autumn, respectively.

3.5.3. Annual AET

The effects of climate change on average seasonal and annual DAET in the basin was investigated under RCP4.5 and RCP8.5 scenarios for the temporal period 1986–2100. AET predictions were made for two time periods: 2041–2070 and 2071–2100. The maximum annual AET for the

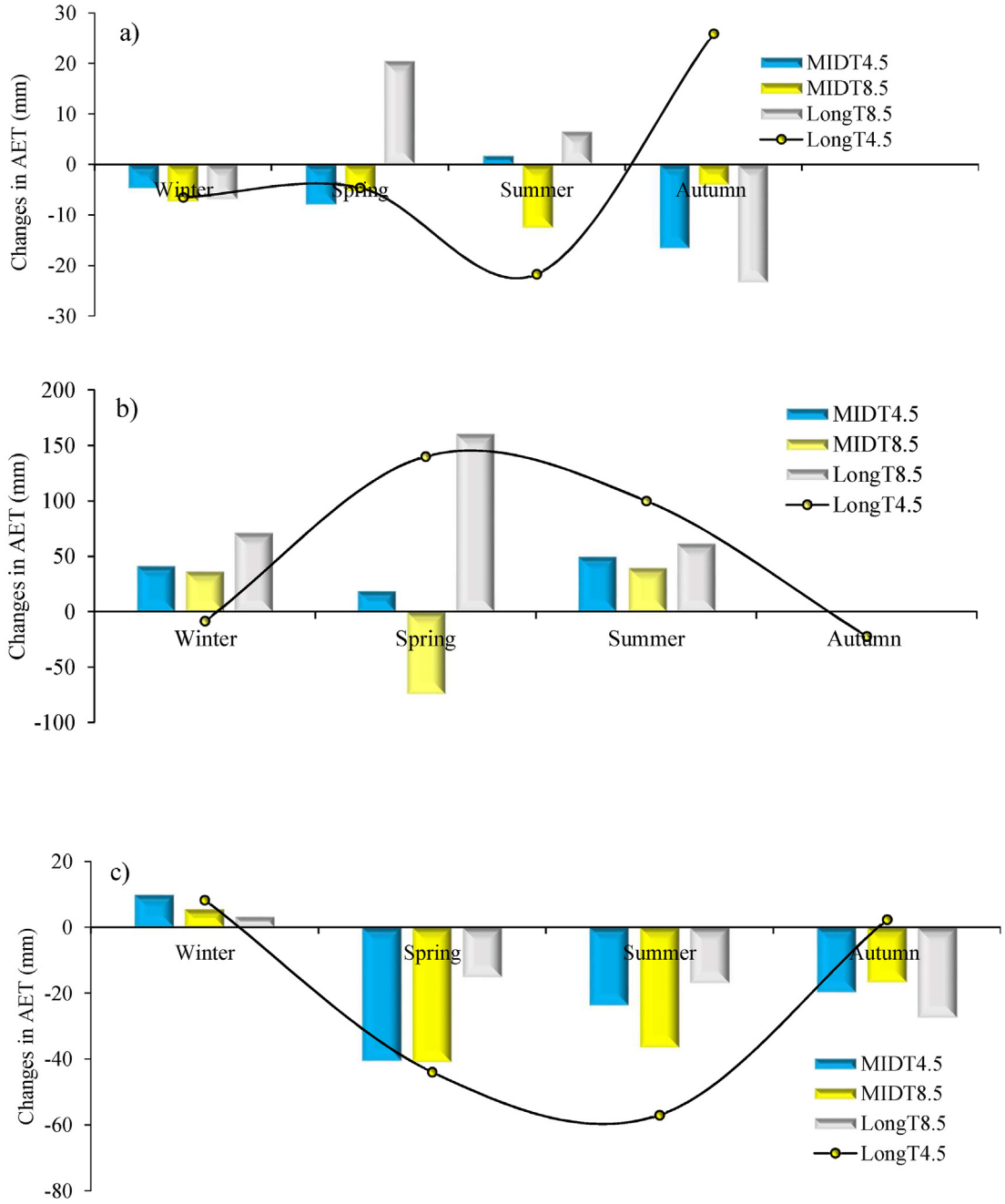

Figure 10. Seasonal actual evapotranspiration (mm). Note: a) refers to the minimum AET, b) refers to the maximum AET, and c) refers to the mean AET.

baseline period (1986–2015) was predicted to be 2815.8 mm/yr; for RCP4.5 scenarios, it was 3019.2 and 3212.1 mm/yr for both periods, and for RCP8.5, this was 3116 and 3352.2 mm/yr, respectively (Figure 11a). The baseline annual AET was 516.6 mm/yr, while the mid-term (RCP4.5 and RCP8.5) and long-term (RCP4.5 and RCP8.5) predicted mean annual AETs of 423.8 and 432 mm/yr, and 429.6, and 438.5 mm/yr, respectively. The minimum annual AET in the basin decreases by 250.2 mm/yr during the baseline, whereas the minimum annual AET is predicted to decrease by 221.7 and 227.3 mm/yr, 223.5 and 241.7 mm/yr, respectively, in the mid-term (RCP4.5 and RCP8.5) and long-term (RCP4.5 and RCP8.5) scenarios.

3.5.4. Changes in annual AET

For both RCP4.5 and RCP8.5 emission scenarios, the mean annual AET may decrease across the specified periods, with the exception of the basin's maximum AET. Between 2041 and 2070, the RCP4.5 and RCP8.5 scenarios predicted a decrease in mean annual AET of 92.8 and 84.6 mm/yr, respectively. During 2071 and 2100, the model predicted a decrease in mean annual AET by 87 and 78.2 mm/yr for both scenarios, respectively (Figure 11b). In the RCP4.5 and RCP8.5 scenarios, the yearly maximum AET was more likely to increase for the entire simulation period in RCP4.5 than in RCP8.5 scenarios (Figure 11b). As a result, the annual maximum AET in that RCP4.5 scenario might increase between 200.1 mm and 299.9 mm in the 2041–2070 and 2071–2100 periods, respectively. In the 2041–2070 and 2071–2100 timeframes, RCP8.5 annual maximum AET usually varies from 400 mm to 540.1 mm. Furthermore, maximum actual evapotranspiration is expected to be significantly higher in the mid-and long-term periods under RCP4.5 and RCP8.5 emission scenarios, respectively.

4. Discussions

4.1. Projected climate changes impressions

In the context of climate change and its consequences, hydro-climatic projections, spatial and temporal distributions of actual evapotranspiration, as well as variability estimations, are crucial for water resource management and development. In terms of seasons, in most parts of the basin, rainfall is intense in April, July and August (Figure 4). The bias-corrected results from the CORDEX climate model ensemble mean show a decrease in annual precipitation and actual evapotranspiration for the study area under both the RCPs, even though seasonal changes do not always show up in the same direction, all models predicted higher temperatures in the future (Figure 13). According to a few climate change studies for Ethiopia, the predicted changes in precipitation and temperature are comparable (Alehu et al., 2021).

4.1.1. Projected precipitation effects

The spatial complexity and changes in climate have a remarkable impact on overall future precipitation patterns. The amount and distribution of future precipitation becomes difficult to determine due to the basin's undulating topographical and geological features. The northern and northwestern highland stations (Hossana and Hulbarag) receive relatively sufficient rainfall in both scenarios. In both scenarios, the

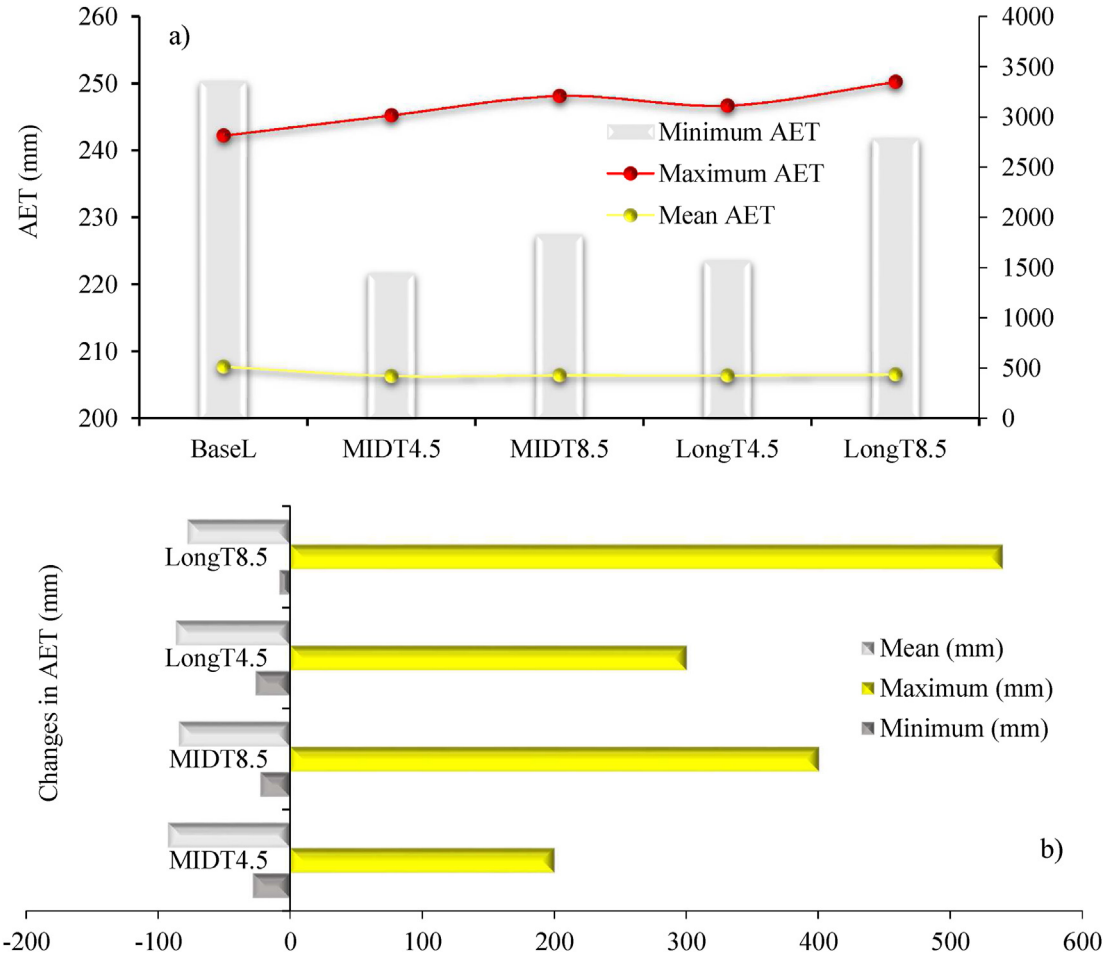

Figure 11. Mean annual AET (mm). Note that a) represents the magnitude of AET for historical and RCP (4.5 and 8.5) scenarios over mid- and long-term periods, b) changes in AET compared to base eras.

central, southeastern, and southernmost stations were predicted to have medium and low to medium rainfall (Alaba-Kulito, Boditi, and Bilate stations). The highest decrease in rainfall was simulated at Hossana station with computed value of 599.98 mm (30.21%) during 2071–2100 with RCP8.5, and the least was observed at Boditi station (3.09 mm) (Figure 6). The unpredictable nature of climate change has a significant impact on the farming community in both the med-term and long-term for both scenarios due to the impact of summer and spring rains on agricultural production. The rain-fed agronomy of the Bilate river basin is likely to be negatively affected by the subsequent decades' decline in rainfall magnitude. Research from the past reveals that climate change is likely to aggravate agricultural system vulnerabilities in the semi-arid regions of Ethiopia, when coupled with non-climatic causes and pressures (Antwi-Agyei et al., 2017; Serdeczny et al., 2017). Lower rainfall and wet/dry period oscillations in coastal towns, lake regions, highlands, and desert and semi-arid plains of Africa's Great Horn, including Ethiopia, will affect the lifestyle of the communities (Osima et al., 2018).

4.1.2. Preview of the projected temperature

According to the RCP4.5 and RCP8.5 scenarios, the predicted maximum and minimum mean annual temperatures show a consistent increase throughout the period of the projected timeframe (Figure 12 a and b). Over the central and lower regions of the Bilate River Basin, the minimum and maximum temperature increase is anticipated (Figure 12). The predictions of the mean annual and seasonal temperatures made by the two RCPs for upcoming, non-overlapping time periods are depicted (Figure 8a–e) and demonstrate a rise throughout the basin. RCP8.5 has a higher seasonal temperature increment than RCP4.5. The average annual and seasonal temperature projections indicate rise over the basin, however summer seasons show less growth than the other seasons (Teshome and Zhang., 2019; Orkodjo et al., 2022; Ukumo et al., 2022). The pace of increase is most likely comparable to the global rate per decade (IPCC, 2007).

The long-term RCP8.5 scenario forecasted a maximum average temperature of 25.38 °C in the lower reaches of the basin due to its low altitude (Figure 13). The minimum average temperature in the northwest highlands, specifically in the Hossana province, was projected, with a predicted value of 14.71 °C during the baseline periods. There may be an increase in the maximum average temperature at the end of the century based on future projections (Feyissa, 2018, Fita and Abate, 2022; Orkodjo et al., 2022). In spite of the rainfall patterns, the average temperature will practically increase throughout the basin and in all seasons (Figure 13a-e). The simulation of temperature and rainfall employing CORDEX regional climate models ICHEC-HIRAM5, MPI-CCLM4, and CNRM-RCA4 demonstrated effectiveness for the accuracy assessment (Elshamy et al., 2009; Worku et al., 2020; Demissie and Sime, 2021; Rahimpour et al., 2021).

4.1.3. Predicted changes in AET

In the Bilate river basin of Ethiopia's Rift Valley system, the effects of climate change-related factors and their retrospective impacts on space-time distributed AET systems are assessed. The hydrologic cycle is likely to proceed in the opposite direction of AET due to changes in CC, future precipitation, and temperature variations. For the 1986–2015, 2041–2070, and 2071–2100 periods for the RCP4.5 and RCP8.5 scenarios, climate data (precipitation and temperatures) are independently

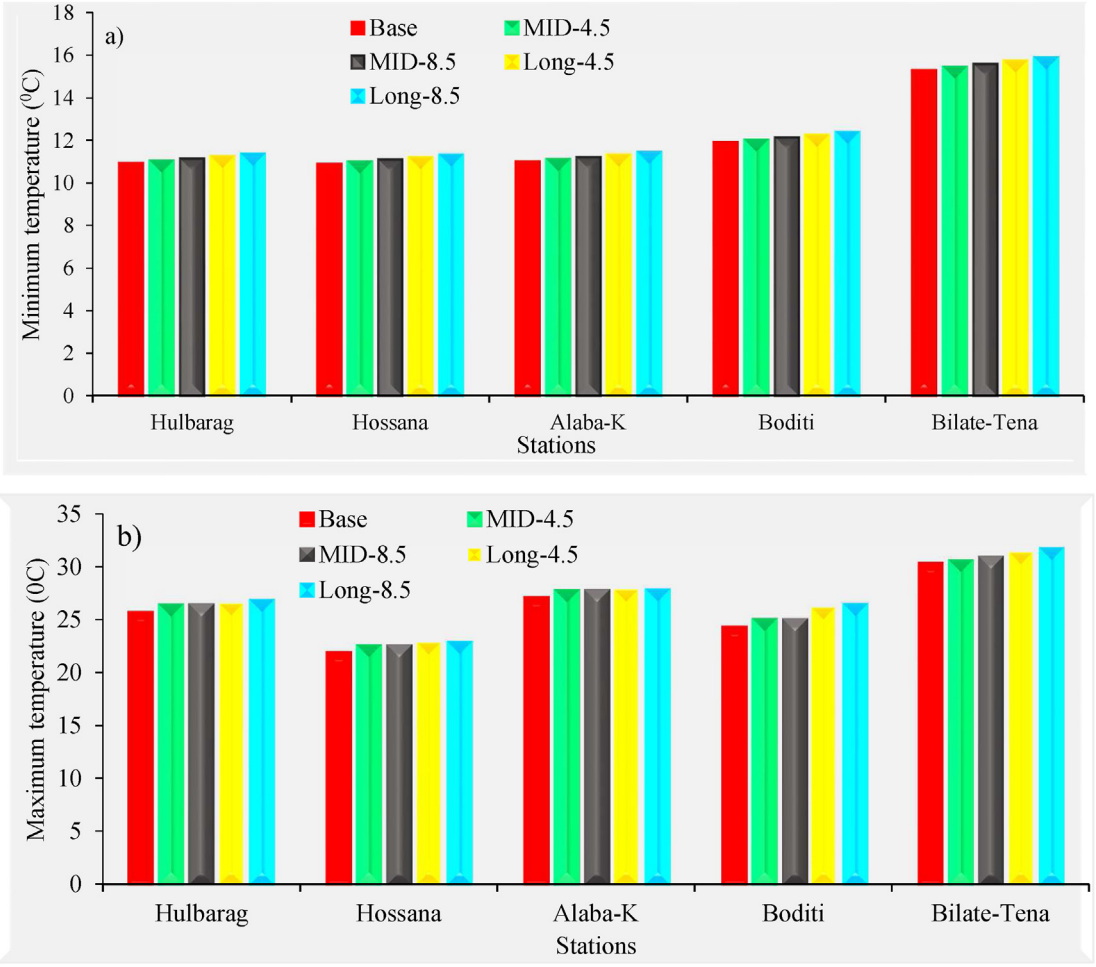

Figure 12. Projected minimum and maximum mean annual temperature in the basin. Noted: a) minimum mean annual temperature, b) maximum mean annual temperature.

derived from the CORDEX Africa program. The WetSpass-M model is used to look at the historical seasonal and annual DAET's spatial and temporal distribution.

The WetSpass-M model's global and local model parameters were examined for their impact on AET variation throughout the referral period. The WetSpass-M model accurately simulated the total surface runoff and base flow statistics after calibration with R^2 values of 0.89 and 0.91 showing strong agreement for the base period (Figure 9 a and b). After calibration, the WetSpass-M model's total surface runoff and subsurface flow outputs were both acceptable. The observed and modeled flows are not well matched, as shown in the graph. In some months, such as April, June, July, August, and December, there is a visible gap between the two graph lines in both surface runoff and subsurface (base flow). Since, the observed discharge data utilized was from 1991 to 2015, and the simulated discharge data was based on climatological data from 1986 to 2015, there is a discrepancy between the two sets of data on the graph.

With the exception of the basin's maximum AET for both emission scenarios, the mean annual AET may decrease during the indicated periods. The magnitude of AET as a spatial and temporal variation are demonstrated in Figure 14. In the RCP4.5 and RCP8.5 scenarios, the yearly maximum AET was far more likely to increase throughout the computation period in RCP4.5 than in RCP8.5 situations (Figure 10c). Climate change may negatively affect future AET, and Casanueva et al. (2019) predicting that future mean annual AET may decline (Raposo et al., 2013; Moeck et al., 2016; Gemitzi et al., 2017; Kahsay et al., 2018; Saatloo et al., 2019; Atawneh et al., 2021; Hughes et al., 2021; Jannis et al., 2021; Tigabu et al., 2021).

4.2. Potential impacts of climate changes

The primary reason for increasing maximum actual evapotranspiration changes in the seasonal distribution, intensity, and duration of

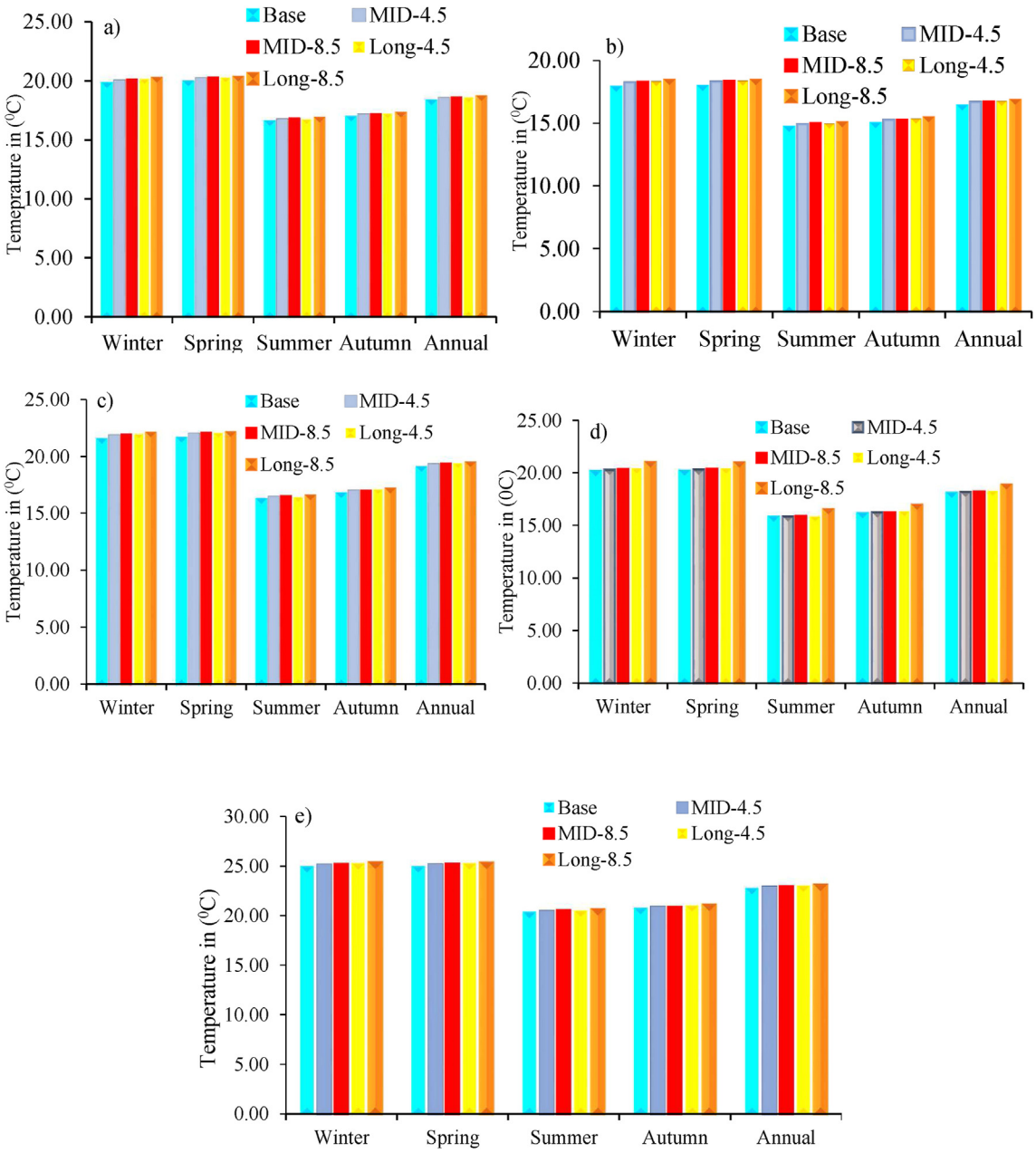

Figure 13. Predicted mean seasonal and annual temperature of in the stations of the basin. Note: a) = Hulbarag, b) = Hossana, c) = Alaba-Kulito, d) = Boditi, and e) = Bilate-Tena weather stations.

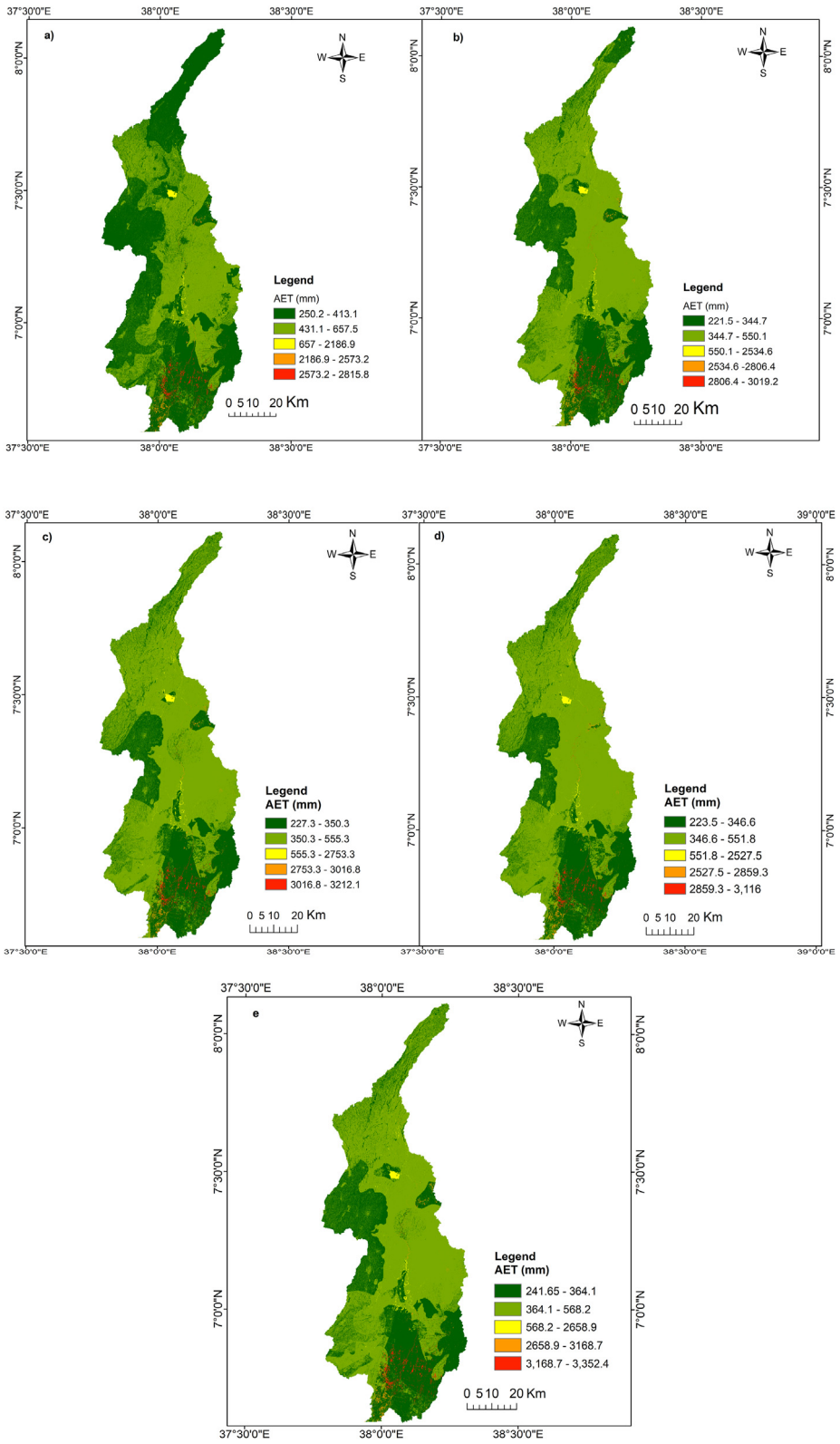

Figure 14. Spatially distributed average annual AET for RCP4.5 and RCP8.5 scenarios during mid-term and long-term periods. Note: a) = base periods, b) = mid-term RCP4.5, c) = mid-term RCP8.5, d) = long-term RCP4.5, e) = long-term RCP8.5.

rainfall, as well as a rise in temperature, all of which are significant changes in the water regime in Ethiopia's Bilate river. Urbanization and agricultural land showed clear expansion trends in Ethiopia's Bilate basin (Mathewos et al., 2019; Alehu et al., 2021; Sulamo et al., 2021). As a result, between 1989 and 2019, agricultural land and settlement in this area increased dramatically with determined values of 1460.3 km^2 (27%) and 131.5 km^2 (2.4%) (Nannawo et al., 2021). Agricultural land expansion, deforestation, and bushlands in this basin affect increased surface-runoff rates in the river system. Surface runoff might be altered by rising urbanization and agricultural land (Abdollahi et al., 2017). In

the coming decades, the mean annual AET will decrease for both RCPs (Figure 11a and b). As illustrated in (Figure 14a-e), locations with higher forest cover can accumulate more water than those with more grass and bushes (Dereje and Nedaw, 2019; Meresa and Taye, 2019).

In the basin, the annualized return AET was determined using the WetSpass-M model simulation with various land use and soil parameter combinations. In both the scenarios (RCP4.5 and RCP8.5), moderate seasonal and annual AET is abundant in water bodies with sandy loam soil texture classes, particularly in the central area and along the Bilate river's waterways. The main reason could be due to high temperatures associated with the lake Abbaya swampland in the basin's southernmost portion, and large rainfall amounts associated with agricultural, grass, and shrub lands in the basin's northern mountainous region. For the base, mid-term, and long-term periods, the lowest AET was recorded in the built-up areas particularly in Hossana, Durame, Angacha and Doyogena towns which are situated in the southwest central area of the basin, barren land, and barren landscapes where clayey soil is predominant (Fig 14a-e) having scanty vegetated land. Urbanization and impervious-layered environments may support an extensive volume of surface runoff rather than topping up groundwater recharge and actual evapotranspiration within the basin (Meresa and Taye, 2019; Fang et al., 2020; Xu et al., 2020). Soil formation and deposition in the area can disturb AET (Kuma et al., 2016; Rukundo and Doğan, 2019). In contrast to the evident decrease in mean annual AET during the computed periods and projected RCPs for the next decades, maximum evapotranspiration shows an increment. Most previous studies on Ethiopia's river basin focused on temporal variations in rainfall-runoff, groundwater recharge, surface water availability and evaluation on past AET (Dile et al., 2018; Kahsay et al., 2018; Alehu et al., 2021; Bekele et al., 2019; Molla et al., 2019; Belihu et al., 2020; Sulamo et al., 2021). The current research strongly advocates at the spatial distribution of AET across seven land cover classes and climate change scenarios. Due of their high canopy interception and transpiration rates, forests had the highest AET rates of all land covers. The environmental conditions and plant types controlled AET variations at the sub-basin scale. It seems that the most influencing factors of evapotranspiration rates are air temperature, radiation, vegetation types, soil moisture, leaf area index and the presence of water on the surface and in the subsurface (Dile et al., 2020; Dong et al., 2022). It is possible for one of these factors to restrict actual evapotranspiration. In this case, lesser precipitation in the southeastern central and lowermost regions of the basin complicates annual mean actual evapotranspiration (Tao et al., 2015; Fang et al., 2020; Liu et al., 2020; Ajjur and Al-Ghamdi, 2021; Tigabu et al., 2021).

5. Conclusions

In this study, the impact of climate change-related variables, as well as their substantial repercussions on space-time distributed AET systems, is explored in Ethiopia's Rift Valley system's Bilate river basin. There is a probable variation in CC, future precipitation and temperature shifts causing the hydrologic cycle to move in the opposite to AET. Climate data (precipitation and temperatures) are taken one by one from the CORDEX Africa program as 1986–2015, 2041–2070, and 2071–2100 periods for the RCP4.5 and RCP8.5 scenarios. To examine the spatial and temporal distribution of average seasonal and yearly DAET, the WetSpass-M model is utilized. During the references period, the sensitivity of global and local model parameters of the WetSpass-M model was investigated to examine the impact on AET variation. After calibration, the WetSpass-M model predicted appropriate total surface runoff and base flow statistics. Overall surface runoff and subsurface flow predictions from the WetSpass-M model were both satisfactory, with R^2 values of 0.89 and 0.91, showing close agreement for the base period. As shown in the graph at some points, the observed and predicted flows are not well matched. There is a discrepancy between the two sets of data on the graph because the observed discharge data used was from 1991 to 2015, while the simulated discharge data was based on climatological data from 1986 to 2015. In RCP4.5 scenario, the annual maximum AET might increase between 200.1mm and 299.9mm in the 2041–2070 and 2071–2100 periods, respectively. RCP8.5 has an annual maximum AET ranging from 400mm to 540.1mm during the periods 2041–2070 and 2071–2100. Under RCP4.5 and RCP8.5 emission scenarios, maximum actual evapotranspiration is predicted to be much higher in the mid- and long-term eras. As a result, water resource planning and management are critical to the system's long-term viability, as well as changes in CC and their implications for AET. According to the data, moderate AET was noted in the water bodies when associated with clayey soil types, particularly in the basin's northern, middle portion specifically around the Boyo marsh area, and southern tip of the lake Abbaya marshlands. For the determined emissions scenarios for the references, mid-term, and long-term periods, the highest AET was comprehended in the forest land environment and tree habitat, where loamy and sandy loam soil is predominant. For long-term water resource allocation, planning, utilization, and management, the basin's expected AET is desirable. The WetSpass-M model outperforms all other models, particularly when the location is inaccessible and data from gauging stations is insufficient.

Declarations

Author contribution statement

Abera Shigute Nannawo: Performed the experiments, analyzed and interpretated the data.

Abera Shigute Nannawo: Evaluated and verified the performance of the model.

Tarun Kumar Lohani: Conceived and designed the experiments.

Abunu Atlabachew Eshete & Abera Shigute Nannawo: Analyzed and interpreted the data.

Abunu Atlabachew Eshete: Wrote the paper.

Funding statement

This research did not receive any specific grant from funding agencies in the public, commercial, or not-for-profit sectors.

Data availability statement

The data that has been used is confidential.

Declaration of interest's statement

The authors declare no conflict of interest.

Additional information

No additional information is available for this paper.

Acknowledgements

The authors are grateful to MoWIE and NMA of Ethiopia who have provided the required data to complete the research paper and Arba Minch University for support on conducting the research.

References

Abdollahi, K., Bashir, I., Verbeiren, B., Harouna, M.R., Van Griensven, A., Huysmans, M., Batelaan, O., 2017. A distributed monthly water balance model: formulation and application on Black Volta Basin. Environ. Earth Sci. 76 (5).

Ademe, F., Kibret, K., Beyene, S., Mitike, G., Getinet, M., 2020. Rainfall analysis for rain-fed farming in the great rift valley basins of Ethiopia. J. Water Climate Change 11 (3), 812–828.

Ajjur, S.B., Al-Ghamdi, S.G., 2021. Evapotranspiration and water availability response to climate change in the Middle East and North Africa. Climatic Change 166 (3–4), 1–18.

Alehu, B.A., Desta, H.B., Daba, B.I., 2021. Assessment of Climate Change Impact on Hydro-Climatic Variables and its Trends over Gidabo Watershed. Modeling Earth Systems and Environment, 2014.
Alemseged, T.H., Tom, R., 2015. Evaluation of regional climate model simulations of rainfall over the Upper Blue Nile basin. Atmos. Res. 161–162, 57–64.
Allen, R.G., Pereira, L.S., Raes, D., Smith, M., Ab, W., 1998. Fao,1998. Irrigation and Drainage Paper No. 56, FAO, p. 300.
Antwi-Agyei, P., Quinn, C.H., Adiku, S.G.K., Codjoe, S.N.A., et al., 2017. Perceived stressors of climate vulnerability across scales in the Savannah zone of Ghana: a participatory approach. Reg. Environ. Change 17 (1), 213–227.
Atawneh, D. Al, Cartwright, N., Bertone, E., 2021. Climate change and its impact on the projected values of groundwater recharge: a review. J. Hydrol. 601 (June), 126602.
Ayele, M.A., Lohani, T.K., Mirani, K.B., Edamo, M.L., Ayalew, A.T., 2022. Simulating 640 sediment yield by SWAT and optimizing the parameters using SUFI-2 in Bilate river of Lake Abaya in Ethiopia. World Journal of Engineering 642.
Batelaan, O., Smedt, F.D.E., 2001. WetSpass : a flexible , GIS based , distributed recharge methodology for regional groundwater modelling, 269, pp. 11–17.
Bekele, A.A., Pingale, S.M., Hatiye, S.D., Tilahun, A.K., 2019. Impact of climate change on surface water availability and crop water demand for the sub-watershed of Abbay Basin, Ethiopia. Sustain. Water Resources Manag. 5 (4), 1859–1875.
Bekele, W.T., Haile, A.T., Rientjes, T., 2021. Impact of climate change on the streamflow of the Arjo-Didessa catchment under RCP scenarios. J. Water Climate Change 12 (6), 2325–2337.
Belihu, M., Tekleab, S., Abate, B., Bewket, W., 2020. Hydrologic response to land use land cover change in the upper Gidabo watershed, Rift valley lakes basin, Ethiopia. HydroResearch 3, 85–94.
Berg, P., Feldmann, H., Panitz, H.J., 2012. Bias correction of high resolution regional climate model data. J. Hydrol. 448–449, 80–92.
Cannon, A.J., Sobie, S.R., Murdock, T.Q., 2015. Bias correction of GCM precipitation by quantile mapping: how well do methods preserve changes in quantiles and extremes? J. Clim. 28 (17), 6938–6959.
Casanueva, A., Kotlarski, S., Herrera, S., Fischer, A.M., Kjellstrom, T., Schwierz, C., 2019. Climate projections of a multivariate heat stress index: the role of downscaling and bias correction. Geosci. Model Dev. (GMD) 12 (8), 3419–3438.
Demissie, T.A., Sime, C.H., 2021. Assessment of the performance of CORDEX regional climate models in simulating rainfall and air temperature over southwest Ethiopia. Heliyon 7 (8), e07791.
Dereje, B., Nedaw, D., 2019. Groundwater recharge estimation using WetSpass modeling in upper bilate catchment, southern Ethiopia. Momona Ethiopian J. Sci. 11 (Issue 1), 37.
Dile, Y.T., Tekleab, S., Kaba, E.A., Gebrehiwot, S.G., Worqlul, A.W., et al., 2018. Advances in water resources research in the Upper Blue Nile basin and the way forward: a review. J. Hydrol. 560, 407–423.
Dile, Y.T., Ayana, E.K., Worqlul, A.W., Xie, H., Srinivasan, R., Lefore, N., et al., 2020. Evaluating satellite-based evapotranspiration estimates for hydrological applications in data-scarce regions: a case in Ethiopia. Sci. Total Environ. 743, 140702.
Dimitriadou, S., Nikolakopoulos, K.G., 2021. Evapotranspiration trends and interactions in light of the anthropogenic footprint and the climate crisis: a review. Hydrology 8 (4).
Dong, Z., Hu, H., Wei, Z., Liu, Y., Xu, H., Yan, H., et al., 2022. Estimating the actual evapotranspiration of different vegetation types based on root distribution functions. Front. Earth Sci. 10, 893, 388.
Eden, J.M., Widmann, M., Maraun, D., Vrac, M., 2014. Comparison of GCM- and RCM-simulated precipitation following stochastic postprocessing. J. Geophys. Res. 119 (19), 40, 11,053.
Elshamy, M.E., Seierstad, I.A., Sorteberg, A., 2009. Impacts of climate change on Blue Nile flows using bias-corrected GCM scenarios. Hydrol. Earth Syst. Sci. 13 (5), 551–565.
Edamo, M.L., Bushir, K.M. a, Ukumo, T.Y., Ayele, M.A., Alaro, M.A., Borko, H.B., 2022. Effect of Climate Change on Water Availability in Bilate Catchment, Southern Ethiopia, Water Cycle.
Eromo, S., Adane, C., Santosh, A., Pingale, M., 2016. Assessment of the impact of climate change on surface hydrological processes using SWAT : a case study of Omo-Gibe river basin , Ethiopia. Modeling Earth Sys. Environ. 2 (4), 1–15.
Fang, D., Hao, L., Cao, Z., Huang, X., Qin, M., Hu, J., Liu, Y., 2020. Combined effects of urbanization and climate change on watershed evapotranspiration at multiple spatial scales. J. Hydrol. 587 (March), 124869.
FAO, 2007. The state of the food and agriculture. In: FAO Agricultur, 38.
Feyissa, G., 2018. Downscaling of future temperature and precipitation extremes in Addis Ababa under climate change. Climate 6 (3), 58.
Fita, T., Abate, B., 2022. Impact of climate change on streamflow of Melka Wakena catchment, Upper Wabi Shebelle sub-basin, south-eastern Ethiopia. J. Water Climate Change 13 (5), 1995–2010.
Gebremeskel, G., Kebede, A., 2018. Estimating the effect of climate change on water resources: integrated use of climate and hydrological models in the Werii watershed of the Tekeze river basin, Northern Ethiopia. Agri. Natural Resourc. 52 (2), 195–207.
Haile, G.G., Kassa, A.K., 2015. Investigation of precipitation and temperature change projections in werii watershed, Tekeze river basin, Ethiopia; application of climate downscaling model. J. Earth Sci. Climatic Change 6 (8).
Gemitzi, A., Ajami, H., Richnow, H., 2017. Developing empirical monthly groundwater recharge equations based on modeling and remote sensing data – modeling future groundwater recharge to predict potential climate change impacts. J. Hydrol. 546, 1–13.
Green, T.R., Taniguchi, M., Kooi, H., Gurdak, J.J., Allen, D.M., Hiscock, K.M., et al., 2011. Beneath the surface of global change: impacts of climate change on groundwater. J. Hydrol. 405 (3-4), 532–560.
Haji, M., Wang, D., Li, L., Qin, D., Guo, Y., 2018. Geochemical evolution of fluoride and implication for F- enrichment in groundwater: example from the Bilate river basin of southern main Ethiopian rift. Water 10 (12).
Hughes, A., Mansour, M., Ward, R., Kieboom, N., Allen, S., Seccombe, D., Charlton, M., Prudhomme, C., 2021. The impact of climate change on groundwater recharge: national-scale assessment for the British mainland. J. Hydrol. 598, 126336.
Hussen, B., Mekonnen, A., Murlidhar, S., 2018. Integrated water resources management under climate change scenarios in the sub-basin of Abaya-Chamo , Ethiopia. Modeling Earth Sys. Environ. 4 (1), 221–240.
IPCC, 2007. Intergovernmental Panel on Climate Change the Physical Science Basis. Cambridge University Press, Cambridge, UK.
Jannis, E., Adrien, M., Annette, A., Peter, H., 2021. Climate change effects on groundwater recharge and temperatures in Swiss alluvial aquifers. J. Hydrol. X 11, 100071.
Jarosław, C., Batelaan, O., 2011. Application of the WetSpa distributed hydrological model for catchment with significant contribution of organic soil. Upper Biebrza case study. Ann. Warsaw Univ. Life Sci. - SGGW. Land Reclam. 43 (1).
Kahsay, K.D., Pingale, S.M., Hatiye, S.D., 2018. Impact of climate change on groundwater recharge and base flow in the sub-catchment of Tekeze basin, Ethiopia. Groundwater Sustain. Develop. 6 (December 2017), 121–133.
Kiesel, J., Gericke, A., Rathjens, H., Wetzig, A., Kakouei, K., Jähnig, S.C., Fohrer, N., 2019. Climate change impacts on ecologically relevant hydrological indicators in three catchments in three European ecoregions. Ecol. Eng. 127, 404–416.
Kumar, H.G., Feyessa, F.F., Demissie, T.A., 2021. Hydrologic responses to climate and land-use/land-cover changes in the Bilate catchment, Southern Ethiopia. J. Water Climate Change 12 (8), 3750–3769.
Kumar, P., Herath, S., Avtar, R., Takeuchi, K., 2016. Mapping of groundwater potential zones in Killinochi area, Sri Lanka, using GIS and remote sensing techniques. Sustainable Water Resour. Manag. 2 (4), 419–430.
Liersch, S., Tecklenburg, J., Rust, H., Dobler, A., Fischer, M., et al., 2018. Are we using the right fuel to drive hydrological models? A climate impact study in the Upper Blue Nile. Hydrol. Earth Syst. Sci. 22 (4), 2163–2185.
Liu, H., Wang, Z., Ji, G., Yue, Y., 2020. Quantifying the impacts of climate change and human activities on runoff in the lancang river basin based on the budyko hypothesis. Water (Switzerland) 12 (12), 1–11.
Mathewos, M., Dananto, M., Erkossa, T., Mulugeta, G., 2019. Land use land cover dynamics at Bilate Alaba sub-watershed, southern Ethiopia. J. Appl. Sci. Environ. Manag. 23 (8), 1521.
McSweeney, C., New, M., Lizcano, G., Lu, X., 2010. The UNDP climate change country profiles. Bull. Am. Meteorol. Soc. 91 (2), 157–166.
Mengistu, D., Bewket, W., Dosio, A., Panitz, H.J., 2021. Climate change impacts on water resources in the upper blue nile (Abay) river basin, Ethiopia. J. Hydrol. 592, 125614.
Meresa, E., Taye, G., 2019. Estimation of groundwater recharge using GIS-based WetSpass model for Birki watershed , the eastern zone of Tigray , Northern Ethiopia. Sustainable Water Resour. Manag. 5 (4), 1555–1566.
Moeck, C., Brunner, P., Hunkeler, D., 2016. The Influence of Model Structure on Groundwater Recharge Rates in Climate-Change Impact Studies.
Molla, D.D., Tegaye, T.A., Fletcher, C.G., 2019. Simulated surface and shallow groundwater resources in the Abaya-Chamo Lake basin, Ethiopia using a spatially-distributed water balance model. J. Hydrol.: Reg. Stud. 24, 100615.
Mutayoba, E., Kashaigili, J.J., 2017. Evaluation for the performance of the CORDEX regional climate models in simulating rainfall characteristics over mbarali river catchment in the rufiji basin, Tanzania. J. Geosci. Environ. Protect. 5 (4), 139–151.
Nannawo, A.S., Lohani, T.K., Eshete, A.A., 2021. Exemplifying the effects using WetSpass-M model depicting the landscape modifications on long-term surface and subsurface hydrological water balance in Bilate basin of Ethiopia. Adv. Civ. Eng. 2021, 20.
Nannawo, A.S., Lohani, T.K., Eshete, A.A., Ayana, M.T., 2022. Evaluating the dynamics of hydroclimate and streamflow for data-scarce areas using MIKE11-NAM model in Bilate river basin, Ethiopia. Modeling Earth Sys. Environ. 1–16.
Navarro-Racines, C., Tarapues, J., Thornton, P., Jarvis, A., Ramirez-Villegas, J., 2020. High-resolution and bias-corrected CMIP5 projections for climate change impact assessments. Sci. Data 7 (1), 1–14.
Nhemachena, C., Nhamo, L., Matchaya, G., Nhemachena, C.R., Muchara, B., et al., 2020. Climate change impacts on water and agriculture sectors in southern africa: threats and opportunities for sustainable development. Water 12 (10), 1–17.
Niang, I., Ruppel, O.C., Abdrabo, M., Essel, A., Lennard, C., Padgham, J., Urquhart, P., 2014. IPCC WGII AR5 Chapter 22. Africa. January, pp. 1199–1265.
Nyenje, P.M., Batelaan, O., 2009. Estimating the effects of climate change on groundwater recharge and baseflow in the upper Ssezibwa catchment, Uganda. Hydrol. Sci. J. 54 (4), 713–726.
Orkodjo, T.P., Kranjac-Berisavijevic, G., Abagale, F.K., 2022. Impact of Climate Change on Future Precipitation Amounts, Seasonal Distribution, and Streamflow in the Omo-Gibe basin, Ethiopia. Heliyon, e09711.
Osima, S., Indasi, V.S., Zaroug, M., Endris, H.S., Gudoshava, M., et al., 2018. Projected climate over the greater Horn of africa under 1.5 ^{0}C and 2 ^{0}C global warming. Environ. Res. Lett. 13 (6).
Rahimpour, M., Tajbakhsh, M., Memarian, H., Aghakhani Afshar, A., 2021. Impact Assessment of climate change on hydro-climatic conditions of arid and semi-arid watersheds (case study: zoshk-Abardeh watershed, Iran). Journal of Water and Climate Change 12 (2), 580–595.
Raposo, J.R., Dafonte, J., Molinero, J., 2013. Assessing the impact of future climate change on groundwater recharge in Galicia-Costa , Spain. Hydrogeol. J. 21 (2), 459–479.
Rukundo, E., Doğan, A., 2019. Dominant influencing factors of groundwater recharge spatial patterns in Ergene river catchment, Turkey. Water 11 (4).

Saatloo, S.M.E., Siosemarde, M., Hosseini, S.A., Rezaei, H., 2019. The effects of climate change on groundwater recharge for different soil types of the west shore of Lake Urmia—Iran. Arabian J. Geosci. 12 (8).
Serdeczny, O., Adams, S., Baarsch, F., Coumou, D., Robinson, A., et al., 2017. Climate change impacts in Sub-Saharan Africa: from physical changes to their social repercussions. Reg. Environ. Change 17 (6), 1585–1600.
Stocker, T.F., Allen, S.K., Bex, V., Midgley, P.M., 2013. Climate Change 2013 the Physical Science Basis Working Group I Contribution to the Fifth Assessment Report of the Intergovernmental Panel on Climate Change. Cambridge University Press.
Sulamo, M.A., Kassa, A.K., Roba, N.T., 2021. Evaluation of the impacts of land use/cover changes on water balance of bilate watershed, rift valley basin, Ethiopia. Water Pract. Technol. 16 (4), 1108–1127.
Tao, X.e., Chen, H., Xu, C. yu, Hou, Y. kun, Jie, M. xuan, 2015. Analysis and prediction of reference evapotranspiration with climate change in Xiangjiang River Basin, China. Water Sci. Eng. 8 (4), 273–281.
Taylor, K.E., Stouffer, R.J., Meehl, G.A., 2012. An overview of CMIP5 and the experiment design. Bull. Am. Meteorol. Soc. 93 (4), 485–498.
Tekle, A., 2015. Assessment of Climate Change Impact on Water Availability of Bilate Watershed, Ethiopian Rift valley basin. IEEE AFRICON Conference.
Teshome, A., Zhang, J., 2019. Increase of extreme drought over Ethiopia under climate warming. Adv. Meteorol.
Tigabu, T.B., Wagner, P.D., Hörmann, G., Kiesel, J., Fohrer, N., 2021. Climate change impacts on the water and groundwater resources of the Lake Tana Basin, Ethiopia. J. Water Climate Change 12 (5), 1544–1563.
Ukumo, T.Y., Lohani, T.K., Edamo, M.L., Alaro, M.A., Ayele, M.A., Borko, H.B., 2022. Application of regional climatic models to assess the performance evaluation of changes on flood frequency in woybo catchment, Ethiopia. Adv. Civ. Eng.
Walraevens, K., Vandecasteele, I., Martens, K., Nyssen, J., Moeyersons, J., et al., 2009. Groundwater recharge and flow in a small mountain catchment in northern Ethiopia. Hydrol. Sci. J. 54 (4), 739–753.
Wang, Z.M., Batelaan, O., De Smedt, F., 1996. A distributed model for water and energy transfer between soil, plants and atmosphere (WetSpa). Phys. Chem. Earth 21 (3), 189–193.
Woldeamlak, S.T., Batelaan, O., De Smedt, F., 2007. Effects of climate change on the groundwater system in the Grote-Nete catchment, Belgium. Hydrogeol. J. 15 (5), 891–901.
Worku, G., Teferi, E., Bantider, A., Dile, Y.T., 2020. Statistical bias correction of regional climate model simulations for climate change projection in the Jemma sub-basin, upper Blue Nile Basin of Ethiopia. Theor. Appl. Climatol. 139 (3–4), 1569–1588.
Xu, C., Rahman, M., Haase, D., Wu, Y., Su, M., Pauleit, S., 2020. Surface runoff in urban areas: the role of residential cover and urban growth form. J. Clean. Prod. 262, 121421.
Yagbasan, O., 2016. Impacts of climate change on groundwater recharge in küçük menderes river basin in western Turkey. Geodin. Acta 28 (3), 209–222.
Yenehun, A., Walraevens, K., Batelaan, O., 2017. Spatial and temporal variability of groundwater recharge in Geba basin, Northern Ethiopia. J. Afr. Earth Sci. 134, 198–212.